

Evaluation of the Tensile Characteristics and Bond Behaviour of Steel Fibre-Reinforced Concrete: An Overview

Mohammed A. Mujalli ^{1,2,*} , Samir Dirar ^{3,1}, Emad Mushtaha ³ , Aseel Hussien ³ and Aref Maksoud ³ 

¹ Department of Civil Engineering, University of Birmingham, Birmingham B15 2TT, UK

² Department of Civil Engineering, College of Engineering, Prince Sattam Bin Abdulaziz University, Alkharj 11942, Saudi Arabia

³ Department of Architectural Engineering, University of Sharjah, Sharjah 27272, United Arab Emirates

* Correspondence: mam162@student.bham.ac.uk

Abstract: Conventional concrete is a common building material that is often ridden with cracks due to its low tensile strength. Moreover, it has relatively low shear strength and, unless reinforced, undergoes brittle failure under tension and shear. Thus, concrete must be adequately reinforced to prevent brittle tensile and shear failures. Steel fibres are commonly used for this purpose, which can partially or fully replace traditional steel reinforcement. The strength properties and bond characteristics between reinforcing steel fibres and the concrete matrix are crucial in ensuring the effective performance of the composite material. In particular, the quality of the bond has a significant impact on crack development, crack spacing, and crack width, among other parameters. Hence, the proper application of steel fibre-reinforced concrete (SFRC) requires a thorough understanding of the factors influencing its bond behaviour and strength properties. This paper offers a comprehensive review of the main factors controlling the bond behaviour between concrete and steel fibres in SFRC. In particular, we focus on the effects of the physical and mechanical properties of steel fibres (e.g., geometry, inclination angle, embedded length, diameter, and tensile strength) on the bond behaviour. We find that the addition of up to 2% of steel fibres into concrete mixtures can significantly enhance the compressive strength, tensile strength, and flexural strength of concrete components (by about 20%, 143%, and 167%, respectively). Furthermore, a significant enhancement in the pull-out performance of the concrete is observed with the addition of steel fibres at various dosages and geometries.

Keywords: steel fibre-reinforced concrete; mechanical properties; pull-out behaviour; bond characteristics; fibre geometry



Citation: Mujalli, M.A.; Dirar, S.; Mushtaha, E.; Hussien, A.; Maksoud, A. Evaluation of the Tensile Characteristics and Bond Behaviour of Steel Fibre-Reinforced Concrete: An Overview. *Fibers* **2022**, *10*, 104. <https://doi.org/10.3390/fib10120104>

Academic Editor: Luciano Ombres

Received: 4 November 2022

Accepted: 29 November 2022

Published: 2 December 2022

Publisher's Note: MDPI stays neutral with regard to jurisdictional claims in published maps and institutional affiliations.



Copyright: © 2022 by the authors. Licensee MDPI, Basel, Switzerland. This article is an open access article distributed under the terms and conditions of the Creative Commons Attribution (CC BY) license (<https://creativecommons.org/licenses/by/4.0/>).

1. Introduction

Concrete is the most popular building material and its use has been on the rise worldwide. In addition to regular applications, higher ductility and energy absorption capacity are particularly required in various fields such as industrial building floors, highway paving, and bridge decks. Conventional concrete has low tensile strength, ductility, crack resistance, and energy absorption. Internal microcracks are inherently present in concrete specimens and their low tensile strength is attributable to the propagation of these microcracks, ultimately contributing to brittle fracturing. Consequently, improving the brittleness and reducing the possible weaknesses of concrete is expected to lead to better performance in various applications [1–3]. Concrete, as a brittle material, is considered to have low post-cracking strength and ductility. In plain concrete, cracks occur when the primary tensile stresses of plain concrete exceed the tensile strength of concrete. In this context, incorporating short fibres into the concrete matrix can reduce microcracking, reduce localised macrocracking, and improve post-cracking strength and ductility [4,5]. Nevertheless, the inclusion of fibres has a slight effect on the concrete's performance before cracking. Short and discrete fibres have been used to strengthen brittle materials for thousands of years.

Different sorts of fibres, whether metallic or polymeric, such as steel fibres, glass fibres, nylon, and polypropylene (PP), have been used in concrete mixtures [2,3].

Bonding can be defined as the shear stress that allows concrete and reinforcement bars to join together [6,7]. Concrete and reinforcement bars can deform at various reinforced concrete levels, due to applied loads, corrosion, high temperature, creep, and shrinkage. As a result of the deformations between the concrete and the reinforcement bar, the stress is transferred through the bond between the two materials. These bonds are the basis for the reinforced action in concrete [8]. The molecular bond strengths that ensure the bond between the steel bar and concrete, the friction force formation between the steel bar and concrete, and the mechanical tread strengths between the deformed steel bar and concrete are the main factors affecting the concrete–reinforcement bond. Due to the first two factors, the bond is known according to the shape in plain steel bars and deformed steel bars can be recognised according to their shape, due to the third factor described above [9].

The bond between concrete and deformed steel bars is affected by the tensile strength of the concrete, the yield strength of the steel, the diameter of the deformed steel bar, the surface geometry of the deformed steel bar, the depth at which the deformed steel bar is embedded into the concrete, the thickness of the concrete cover surrounding the reinforcement, and the position of the steel bar. Pull-out tests are frequently used to determine the bond strength between concrete and deformed steel bars. An axial pull-out load is often used to pull out the deformed steel bar embedded in concrete during pull-out tests. The bond stress generated between the concrete and the deformed steel bar can then be measured, using the pull-out load evaluated in such a test [10,11].

Various studies have been conducted to determine how steel fibres affect the bonding between deformed steel bars and concrete matrices. Steel fibres improve concrete's ductile behaviour, reduce crack formation, and improve the mechanical properties. According to various researchers, such factors result in a stronger bond between the concrete and steel bars in SFRCs [12–14]. According to Feng et al. [15], the majority of fibres available for reinforcement are mechanically pre-deformed. Qi et al. [16] and Yoo et al. [17] have reported that steel hooked-end fibres are more frequently used in cementitious composites than any other type of fibre. Consequently, it is critical to comprehend the fundamental processes regulating the bonding of pre-deformed fibres. This analysis aims to provide fundamental knowledge for successful implementation and future research advancement, by better understanding this specific bond mechanism. The qualities of fibres that exhibit differences in shape and geometry are of particular interest. Therefore, in this study, we critically review the effects of various types and shapes of steel fibres on the behaviour of reinforced concrete, as well as investigating the various properties of reinforced concrete after the addition of steel fibres at different dosages. We also highlight the gaps in the relevant research that deserve further investigation.

2. Bond Behaviour of Steel Fibre Reinforced Concrete

As previously mentioned, the use of fibres to improve the properties of brittle materials is a very old practice. The straight form of steel fibre was developed as a new form in the early 1960s [18–20]. The friction between the concrete and the fibre defines the fibre's bonding behaviour. Consequently, a rectangular segment with a higher aspect ratio may perform better in terms of bonding [21]. The key role of steel fibres in the concrete matrix is to aid in mitigating the propagation of microcracks [22]. There are two scenarios in which fibres can fail in the matrix. The first is fibre fracture and the second is fibre pull-out from the concrete matrix. As it is more ductile and serves as an energy absorber, the second scenario is preferred. In other words, hooked-end and crimped fibres can bend considerably and yield, allowing the fibre to be pulled out [23]. Consequently, this phase will consume a significant amount of energy. The bond between the steel fibre and the concrete influences the failure form [24].

The bonding features amongst steel fibres or steel bars in the concrete matrix are critical to the success and effectiveness of any reinforced composite material [10]. The behaviour

of steel fibre-reinforced concrete (SFRC)—such as conventional reinforced concrete (RC) reinforcing bars—is strongly influenced by the interface conditions [25,26]. In general, the interfacial bond allows stress to be transmitted from the fibres to the concrete matrix and vice versa [27]. Another critical point amongst SFRC and RC is that steel bars or fibres in concrete cover the weakness under stresses. The fact that reinforcing fibres—unlike reinforcing bars—are not continuous, allows for a significant variance. A significant difference is that, in RC, plastic hinge failure is more common, while steel fibres are typically pulled out before hinges can shape [10,11].

The bonding mechanisms in SFRC are complex and varied [28], due to the involvement of many bond elements and their combined action. The relevant definitions include physical and chemical adhesions among the fibres and matrix, friction, fibre–fibre intersection, and mechanical components within geometric deformations in hooked-end, crimped, and twisted fibres [29]. Consequently, numerous studies have examined the mechanisms described above. Yoo and Choi [17] have reported successful attempts to increase bond-slip resistance by mechanically deforming fibres. Cunha et al. [30], Aslani and Nejadi [31], and Abdellah et al. [32] have investigated the impact of fibre geometry on the bond-slip features of SFRC. After fracturing, the interfacial interaction of SFRC between the steel fibres and the matrix played a more significant role in RC members than steel bars [33]. In an uncracked composite, stress is transferred primarily through the frictional bond at the interface from the matrix to the fibre's longitudinal axis. The load is transferred to the fibres that span the break as the matrix cracks [34]. The tension can be passed back into the uncracked parts of the matrix, due to the strong mechanical bond. This bond also prevents the fibres from pulling away from the matrix. As a result, one of the most critical factors determining the process and failure modes of composites is the bond quality [35].

3. Types of Bond

Due to differences in surface preparation, concrete materials, applications, and curing processes, the bond features in interface zones are among the most critical areas in the concrete matrix. The type of stress transferred across the interface in SFRC and RC can characterise the bonds between fibres, steel bars, and concrete constituents. If the direct tensile stress (P/A_f)—where A_f is the section area of steel fibre and P is the applied pull-out force—is less than its ultimate value, the bond will resist both shear and strain at the interface through the transfer of direct tensile stress in the fibre. Therefore, two types of bonds are defined, based on the level of stress transmitted through an interface: tensile bonds and shear bonds [36,37].

3.1. Shear Bond

A shear bond is responsible for the load transfer parallel to the longitudinal axis of the reinforcement, which can be rebars or steel fibres. In an uncracked composite, a shear bond transfers stress from the matrix to the reinforcement. When the matrix cracks and the load is carried by the fibres bridging the crack, the shear bond allows the load to be moved back into the uncracked sections of the matrix [38,39]. Shear bonds also protect the reinforcement against the pull-out from the matrix, causing it to be one of the most critical factors affecting the mechanism and failure modes of composites. Consider a hooked-end fibre embedded in a concrete matrix subjected to an axial tensile load, as shown in Figure 1a. The applied pull-out force (P) is reacted by an interfacial elastic shear stress (τ_e), as shown in Figure 1b. This shear stress τ may refer to the outer surface area (A) of a length τ of fibre. The elastic shear bond (including any adhesion) and the frictional shear bond can transfer stresses acting along with the interface. Whenever the elastic shear stresses at the reinforcement interface and the matrix exceed the interface bond strength, the bond becomes frictional and the adhesion is broken [40,41].

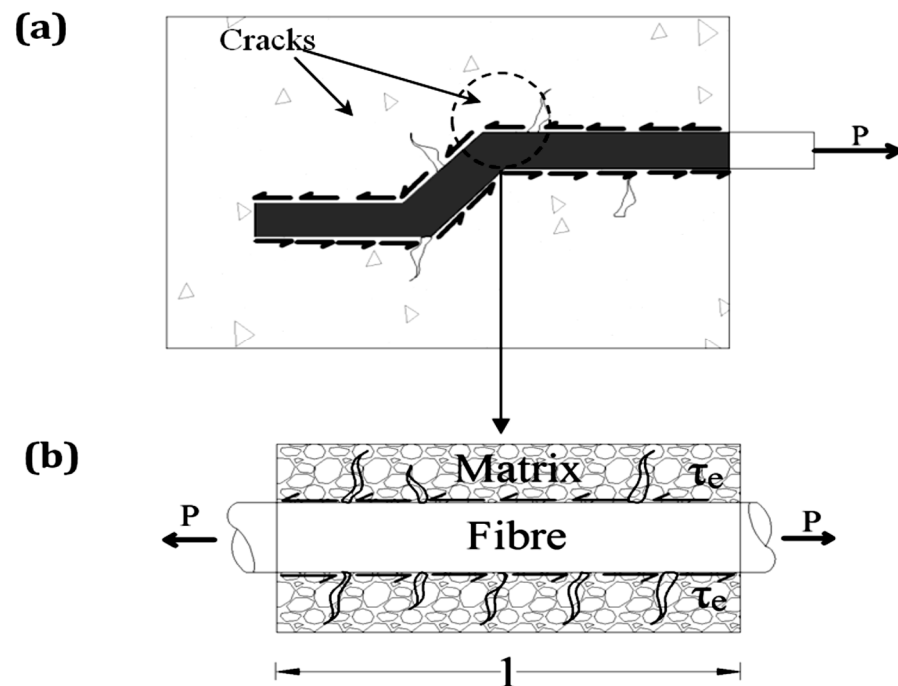


Figure 1. Interfacial shear under axial force: (a) consider a hooked-end fibre embedded in a concrete matrix subjected to an axial tensile load; and (b) the applied pullout force P is reacted by an interfacial elastic shear stress τ_e [40].

When an elastic shear bond occurs at an interface, shear stresses are directly related to the relative slip between the reinforcement and the matrix and the shear stress does not exceed the bond's strength. According to Bandelt and Frank [42], when the elastic band is dominant, the longitudinal displacements of the fibre and matrix at the interface remain compatible. As displacement compatibility implies zero slip, no shear stresses form at the interface, implying an infinitely large bond modulus. Moreover, the frictional shear bond resists displacements parallel to the fibre's length and may or may not be affected by local slip. The tension is independent of the slip if the frictional bond is plastic. The frictional bond is defined by an initial value of the bond (known as the bond strength), which must be exceeded in order for the elastic bond to break and frictional stress to occur [43].

3.2. Tensile Bond

Tensile bonds resist displacement due to forces acting perpendicular to the interface. An unbroken interfacial elastic bond limits the lateral contraction of the fibre. A natural force (N) is induced, as seen in Figure 2, causing the fibre to pull laterally on the matrix along the interface. When N is greater than the pull-out force (P), N must be measured to determine the probability of tensile failure in the matrix [40,44]. The modes of failure in the matrix are typically reduced for a matrix containing a high volume of fibres distributed with random orientations. A supporting column with a small section field, on the other hand, may be vulnerable to transverse tensile failure. Moreover, the tensile modes of failure must be taken into account from a broad perspective. Figure 3a depicts an arbitrary series of fibres, in which a brittle tensile failure under P will follow a primarily perpendicular path amongst them. In this case, fibres aligned with P will be superior to those aligned with N . As shown in Figure 3b, unidirectional reinforcement with fibres running parallel to P is the best way to offset tensile failure from P . However, it will be unsuccessful in resisting tensile failure between fibres under N . As both P and N are present during pull-out, random orientation is the best option, as certain internal fibres are in their best positions to avoid both N and P [40,44,45].

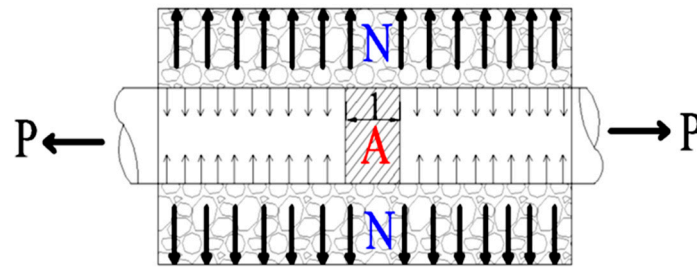


Figure 2. Normal reactional force (N) under pull-out force (P) [40].

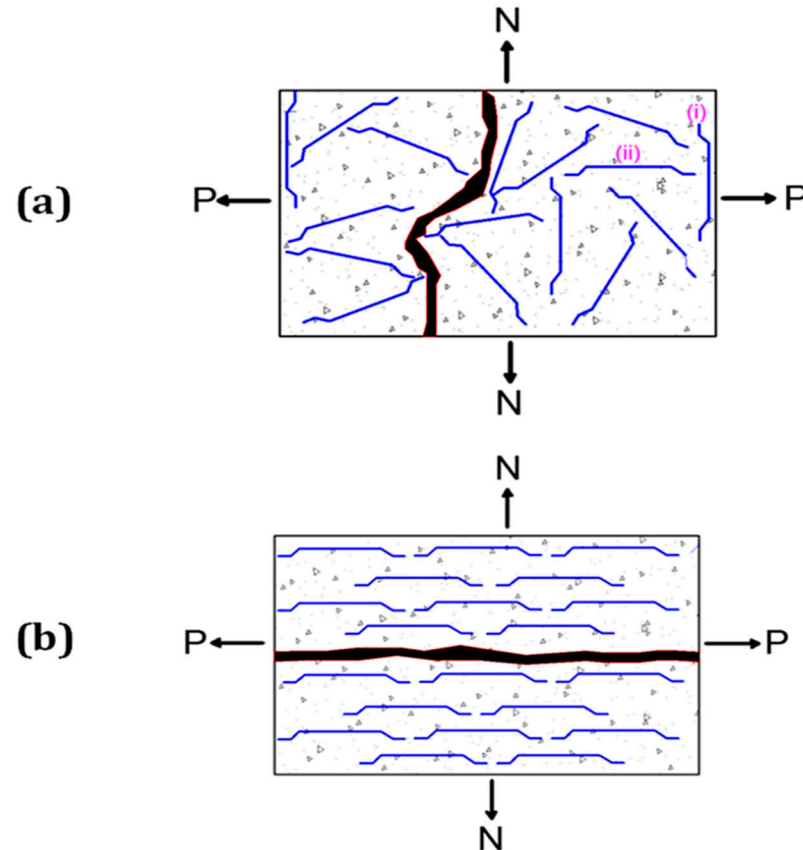


Figure 3. The arrangement of fibres in the matrix: (a) random three-dimensional fibre distribution with optimum orientations (i) and (ii); and (b) unidirectional distribution [40].

4. Fibre–Matrix Interfacial Transition Zone

Generally, the adhesive/ chemical bond in reinforced composites forms a mutual interface between the reinforcement and the surrounding matrix [46,47]. The transfer of stress between the fibre and the surrounding matrix is accomplished in a reinforced concrete composite when the bond serves as an interfacial transition zone (ITZ) [48,49]. The interfacial properties amongst the fibre and concrete matrix significantly impact the efficiency of fibres in transmitting applied stress [50]. Consequently, the bond strength inside the ITZ substantially impacts the tensile response of composites [51]. The transition zone between fibres and the matrix in a cementitious composite is the weakest area among the components governing composite properties, due to its porous nature [52]. The microstructure of the ITZ between the fibre and the matrix is very similar to that of the cement paste–aggregate bond, both of which have high porosity and a high calcium hydroxide $\text{Ca}(\text{OH})_2$ content [53]. A typical interfacial transition zone between a steel fibre and matrix constituents is shown in Figure 4. As shown for the CH layer, local bleeding around fibres results in a less dense dispersion of particles packed around the fibre in the fresh state. The blank areas become

partially filled with hydration products due to inefficient cement particle packing [54]. The microstructure of the matrix in the vicinity of the inclusion in a cementitious composite with aggregate and fibre addition can differ from that of the bulk cement matrix [55,56]. Therefore, the annular cement paste matrix has a greater porosity than the bulk cement pastes. Consequently, the toughness and strength of the ITZ are slightly lesser than those in bulk cement pastes.

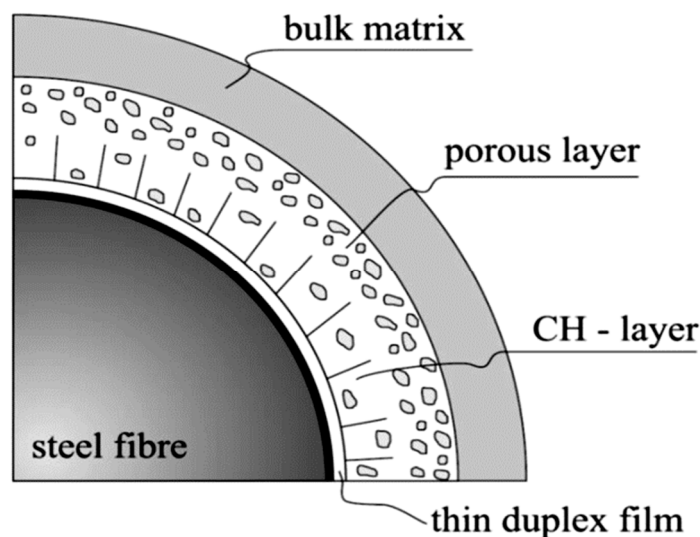


Figure 4. Transverse cross-section of the interfacial zone in the matrix (ITZ) between fibre and matrix [49].

As previously mentioned, the fibre is encircled by an ITZ that is chemically and mechanically distinct from the bulk. This ITZ is measured in tens of micrometres, which is the same size as the hydration products in the cement matrix. Calcium–silica or calcium–alumina hydrates (C-S-H and C-A-H gel), CH, unhydrated clinkers, and pores are the five major hydration products in the hardened matrix. Compared to the bulk matrix, the microstructure of the ITZ around fibres is distinguished by a lower proportion of clinkers and higher proportions of C-S-H gel and CH [41,54]. Microscopic studies have revealed that the ITZ region has smaller clinker or CH grains, due to a higher water/cement ratio and more porosity. Therefore, the matrix’s bond to the fibre surface becomes weaker. The wall effect refers to the effect of a rigid obstacle created by the fibre in the matrix. The key difference between the ITZ and the bulk cement matrix, from a micromechanical standpoint, is the porosity, which decreases the modulus of elasticity in the ITZ [57,58]. The ITZ has an irregular thickness, proportional to the fibre width [59].

Scanning electron microscopy (SEM) is one method that can be used to investigate the ITZ in the fibre matrix [60]. Both phases can be differentiated by the contrast on the scans. The steel fibre, with the highest atomic ratio, is indicated by a white colour, while the other phases are dark grey. As shown in Figure 5, unhydrated clinker particles are the lightest grey particles in the hydrated matrix. Due to a locally higher water/cement (w/c) ratio and more pronounced hydration of these stages, the ITZ zone has a lower percentage of clinkers. Higher w/c ratios, on the other hand, result in increased porosity in the ITZ, which can also be seen in the images [49,51]. Figures 5 and 6 illustrate different aspects of ITZs in SFRC, indicating the porosity, phase distribution, and estimated width of the ITZ in the matrix. Densification of the ITZ is the most successful of the numerous attempts to increase the hardness of the transition region. This can be accomplished by lowering the water/binder ratio or using micro-fillers (e.g., silica fume and fly ash). Although ITZ density is a significant parameter, it does not fully improve interfacial bond power. Comparing aggregate voids and the lack of porosity in steel fibres imposes a limit on the hardness increase in the ITZ [46].

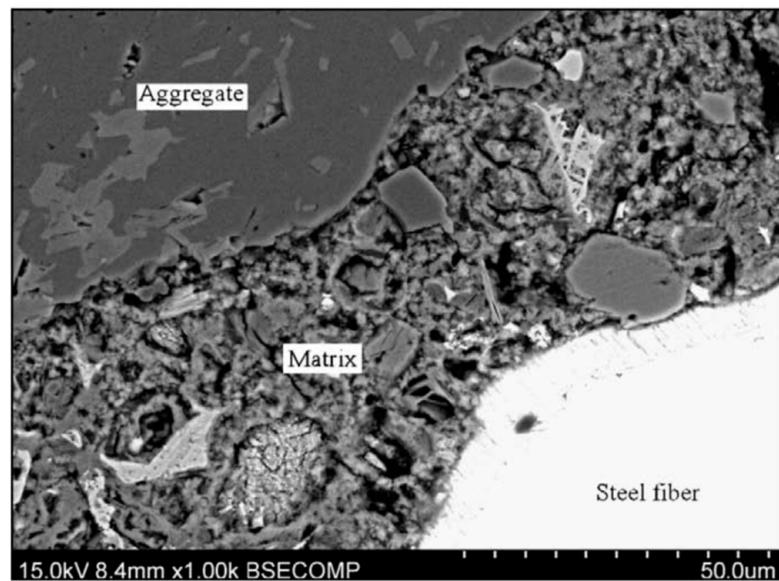


Figure 5. SEM image of steel fibre–matrix interfacial zone in the matrix (ITZ) [46].

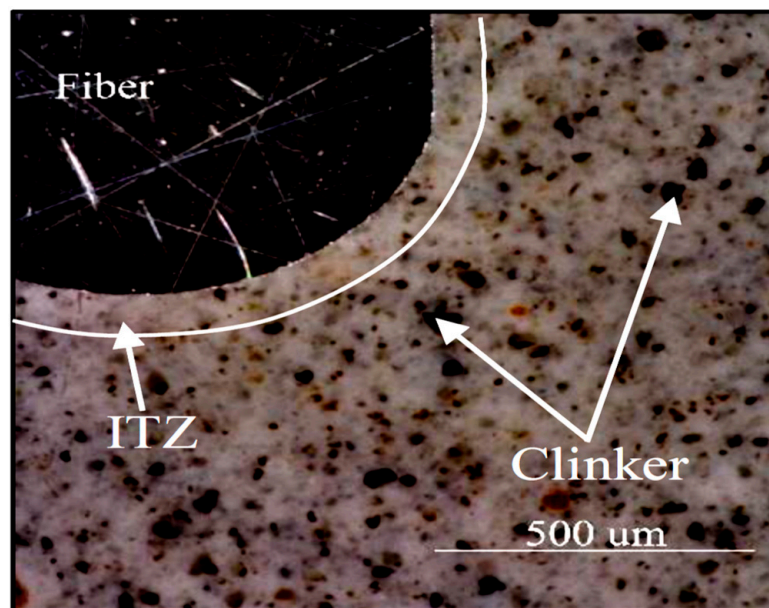


Figure 6. Light microscopy image of steel fibre–matrix interfacial zone in the matrix [51].

5. Factors Affecting Bond Behaviour

The main advantage of incorporating steel fibres into concrete is to improve the quasi-brittle material's post-cracking behaviours, such as durability or energy absorption, especially under stress, as fibres that cross cracks transfer stresses through them, delaying crack opening and propagation. This is accomplished by deforming and/or pulling the fibre out of the crack. The fibre–matrix bond characteristics, which are primarily governed by fibre properties such as geometry, strength, and dimension, as well as matrix strength, the properties of the fibre–matrix interface zone, and the fibre orientation with respect to the loading direction, determine the bridging efficiency or ability of a single fibre [61–64].

5.1. Fibre Geometry

Steel fibres used in concrete composites can be categorised into deformed and undeformed fibres based on their shape, as shown in Figure 7. Straight steel fibres are uncommon in practice and almost all commercially available fibres at present have a

mechanically pre-deformed geometry [65]. The primary reason for mechanically deforming fibres is to provide mechanical anchorage or bonding within the cementitious matrix [66,67]. Deformation can occur at the fibre ends (e.g., hooks, paddles, buttons) or along the length of the fibre (e.g., indented, crimped, and polygonal twisted fibres). The frictional component of a bond controls the pull-out behaviour of straight steel fibres, whereas the mechanical anchorage component controls the pull-out behaviour of a deformed fibre. Therefore, researchers have recommended the use of deformed steel fibres, such as hooked-end fibres, to improve bond behaviour between fibres, matrix constituents, and even steel bars in RC [68].

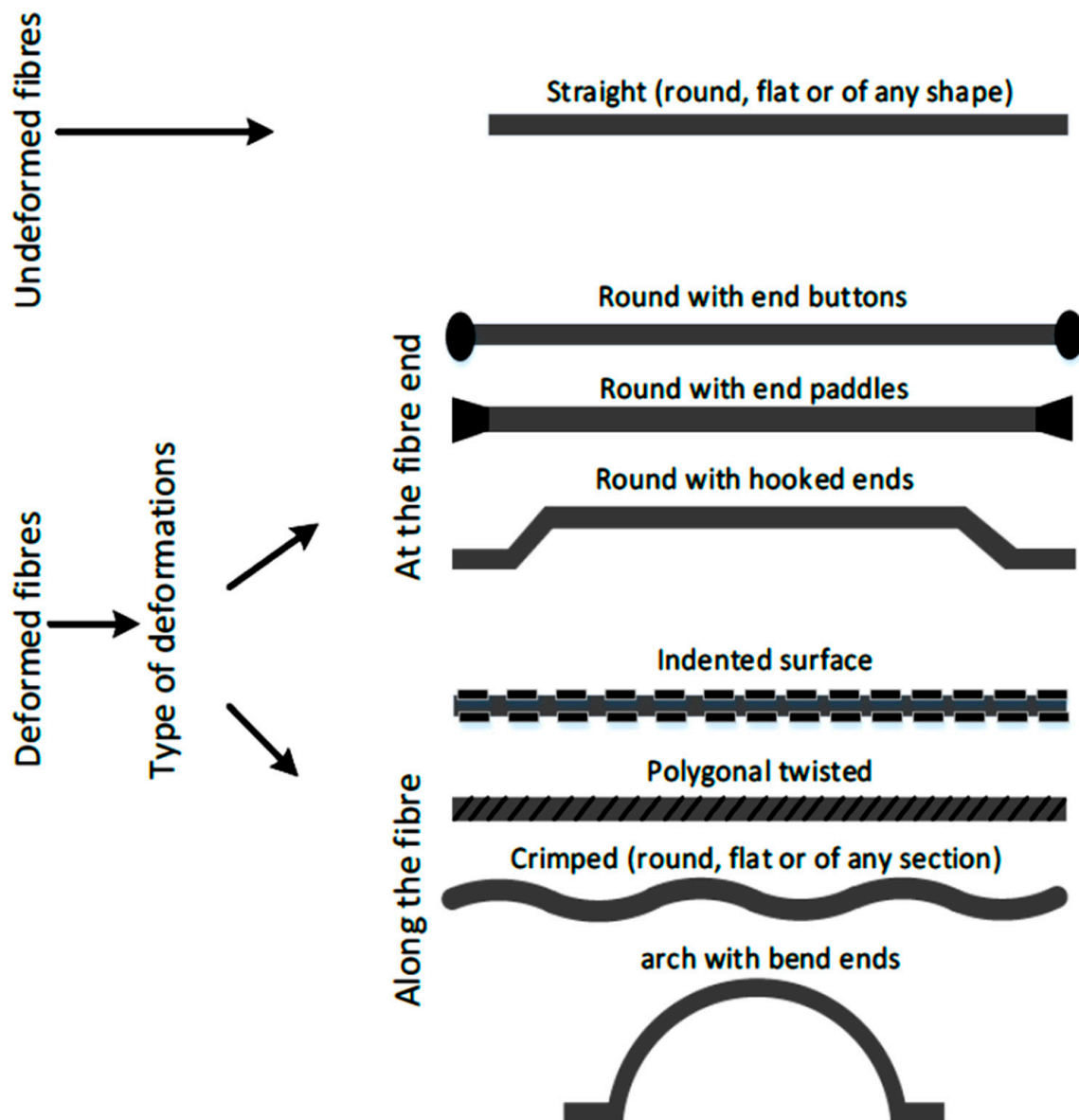


Figure 7. Various steel fibres, categorised according to their geometric shape [40].

Another significant factor in achieving a solid bond and improved SFRC efficiency is the shape of the fibres. Shorter fibres have been shown to increase overall response in many studies [69,70]. Shorter fibres require a slightly higher fibre amount to attain the same fibre content for the same fibre aspect ratio; this larger number of fibres will enhance crack bridging and stress transfer through the cracks. According to numerous reports, steel fibres appear to be pulled out of the matrix, rather than rupturing at the onset of failure [69,71]. Accordingly, the mechanical anchorage provided by deformed

fibres is critical in SFRC performance. Straight fibres with end-hooks have been used in recent experimental studies and constitutive model growth [72–74]. The mechanical anchorage contributions of various types of deformed fibres vary significantly, due to differences in their geometry. These variations significantly impact the fibre pull-out force and, consequently, the tensile response of SFRC [12,19]. Extensive pull-out experiments have been performed to explain the influence of fibre geometry on the pull-out performance of deformed fibre [75–78]. Despite this, it seems that the bonding mechanisms underlying deformed fibre pull-out behaviour are still unclear at present.

5.2. Fibre Volume Fraction

The fibre volume fraction (V_f) is one of the main variables affecting the performance of SFRC. Increases in the fibre volume fraction have been shown to enhance durability, ductility, and toughness in various stress-critical tests, including flexural, uniaxial direct tension, and direct shear tests [79,80]. More fibres are likely to intersect cracks as the fibre content increases, enhancing the capability of the matrix to link cracks and improve post-cracking performance. Toughness—defined as the area under the load–deflection diagram—was dramatically enhanced with increased fibre material content, according to Anbukarasi and Kalaiselvam [81]. This resulted in a considerable rise in concrete ductility, with a slight increase in strength. It was also discovered that increasing the fibre content from 0.5 to 1.0% increased the uniaxial tensile toughness of concrete from 1.8 to 2.7 times that of plain concrete [82].

Increases in the fibre volume fraction often increase the normalised peak shear stress in direct shear tests. In a study, specimens with a medium concrete strength and 0.5, 1.0, and 1.5% fibre volume fractions demonstrated a 60% improvement in the normalised peak shear stress, compared to plain concrete [79]. A high fibre volume fraction can induce strain-hardening behaviour, which is beneficial when the concrete's maximum tensile stress exceeds the first cracking stress. Although the exact fibre content needed for strain-hardening depends on the other properties of the fibres, some studies have found that 1.5% fibre volume may be adequate [69,83]. Increasing the fibre volume fraction improves the compressive post-peak response of concrete to improve the tensile response [84]. The pre-peak division of the compressive stress–strain correlation improves with a rising fibre content, resulting in a slightly higher elastic modulus [69]; this increase is primarily due to the higher elasticity modulus of steel fibres. SFRC, on the other hand, has a lower elasticity modulus than non-fibrous concrete [85]. This is because SFRC uses less coarse aggregates than non-fibrous concrete [69]. It has been reported that the addition of steel fibres increases the compressive strength by only 0–15% [86].

Furthermore, as the steel fibre content increases, the strain corresponding to the highest compressive strength increases, resulting in greater energy absorption ability. Toughness and pressure at high stress are inversely proportional to fibre volume fraction [87]. Steel fibres, on the other hand, significantly strengthen the descending branch of the compressive stress–strain relationship. A high fibre volume fraction results in a flatter descending branch, which improves durability and ductility significantly. Several studies have been conducted to determine the effect of the fibre volume fraction on the bonds between steel fibres, the concrete matrix, and steel bars in RC structures [88]; their findings revealed that up to 2% of steel fibres could significantly improve SFRC and RC bonding.

Despite the benefits of increasing the fibre content, the maximum fibre volume fraction should be limited, due to workability issues and fibre saturation. High fibre content reduces the amount of paste volume fraction available for the free movement of coarse aggregates and fibres, reducing the workability of fresh SFRC [89]. Consequently, processing SFRC with a high fibre content often necessitates unique mixing and placement techniques [1]. Although the maximum fibre content for adequate workability varies, depending on various factors such as placement conditions, conventional reinforcement ratios, concrete mix composition, and fibre properties, the ACI Committee 544 (1993) has recommended a maximum fibre volume fraction of 2.0% for conventional SFRC [90]. If tiny steel microfibres

are used, the fibre content may range from 5.0 to 9.0%, resulting in what is known as an ultra-high-performance fibre-reinforced concrete (UHPFRC) [91]. It is interesting to note that, for conventional SFRC, there could be a point—known as the fibre saturation point—at which any improvement in fibre content would result in marginally improved behaviour. Some studies have suggested that this point may be in the range of 1.0–1.5% [54,92].

5.3. Fibre Aspect Ratio

The fibre aspect ratio—defined as the fibre length to fibre diameter ratio—significantly impacts the effectiveness of fibre reinforcement and matrix bond behaviour. Under the same fibre volume fraction, a higher aspect ratio results in a larger fibre surface area, which further develops the bond amongst the matrix and fibres, resulting in a stiffer matrix and superior composite behaviour [93]. Cao and Yu [23] have found that fibres with greater aspect ratios (equal diameter but varying in length) produced an SFRC mixture with a marginally higher strength but significantly higher toughness in flexural and uniaxial tension tests. Interestingly, Li and Xu [82] studied fibre aspect ratios in the range from 25 to 100 and found that the improved tensile response from higher aspect ratios is only valid up to an aspect ratio of 75; after that, the tensile response deteriorated with any further increase in the aspect ratio. Khaloo and Kim [79] have conducted a direct shear test and found that the normalised shear intensity and maximum displacement increased as the aspect ratio increased. Additionally, cylinder compression experiments using fibres with a higher aspect ratio have shown better post-peak responses, resulting in substantial improvements in durability and ductility [94,95].

5.4. Fibre Orientation

Fibre orientation is a complex yet essential factor to measure. Steel fibres are most efficient whilst closely aligned parallel to tensile stresses and least effective when aligned perpendicular to the direction of tensile stresses. Due to the embedment length of the fibres and the number of fibres crossing a crack decrease as the fibre angle becomes more oblique to the direction of the tensile tension. The efficiency of random fibre orientation lies somewhere in the middle of the two limiting conditions. Several studies on fibre orientation and its influence on fibre quality in SFRC modelling, using a so-called fibre orientation factor, have been carried out [96,97]. This factor typically considers the fibre orientation angle, fibre dimensions, and member dimensions [98]. This element is the average ratio of the expected fibre length in the tensile stress direction to the fibre length itself for all possible fibre orientations.

As the fibres in fibre-reinforced cementitious composites are uniformly distributed and oriented in different directions, not all fibres will lie in the same direction as the applied load [99]. A complex stress condition applies to a fibre inclined to the loading direction, instead of a simple tensile pull-out load for an aligned fibre. The bond mechanisms that control the pull-out force versus the slip response of inclined fibres differ from those tested experimentally on aligned fibres [100]. In addition to the normal de-bonding and friction at the fibre–matrix interface, the inclined fibre introduces fibre bending and local friction effects at the exit points [9]. Consequently, the pull-out resistance of some inclined fibres can be significantly increased. In their studies, Nieuwoudt and Boshoff [101] and Marcos-Meson and Solgaard [102] have demonstrated that the pull-out power of inclined fibres is greater than that of aligned fibres at an optimal inclination of from 0° to 20° (as shown in Figure 8). Due to the bending impact and the concentration of frictional stress at the fibre's exit point, inclination angles greater than 30° increase the likelihood of fibre rupture and matrix spalling. Another explanation could be the strength difference between a low-strength matrix paired with a high-tensile strength fibre or vice versa [103].

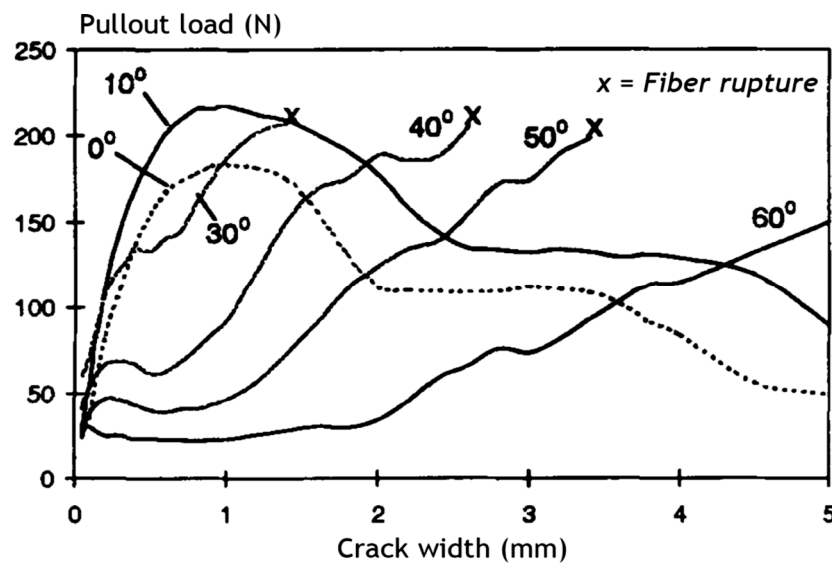


Figure 8. Pull-out behaviour of hooked-end steel fibres at different inclination angles [103].

5.5. Fibre Embedded Length

It is commonly understood that increasing the embedded length of fibres in an SFRC matrix will improve the pull-out resistance [80]. Although this statement appears to be true for straight fibres—as a longer embedded length results in a greater area of the fibres in interaction with the concrete matrix—it rarely applies to deformed fibres such as hooked-end fibres [104]. A greater pull-out force for a smaller embedded length can be applied for identical hook-end geometry. The pull-out resistance—expressed in terms of the plastic deformation of the fibre’s hook—is higher than that provided by a frictional bond along the embedded length, thus explaining this behaviour. Complete plastic deformation and straightening of the hook are impossible in a test with an embedded length shorter than the hook length. Consequently, the embedded length must be greater than the hook length, in order to ensure that the mechanical anchorage portion is fully utilised during the test [105,106].

5.6. Matrix Strength

The bond behaviour and pull-out response of SFRC are significantly influenced by the mechanical properties of the matrix, such as its compressive and tensile strengths. Although it is well-understood that a greater compressive strength of concrete results in a greater first-crack tensile strength, the compressive strength of the matrix does not affect the post-cracking behaviour of concrete [107]. While an advanced concrete strength will improve the bond strength amongst the fibres and the concrete matrix, the steel fibres also introduce greater interfacial shear stresses at the early stage of crack formation, due to the complex first-cracking strength. Consequently, bond-slip can arise before the fibre can be completely de-bonded, causing post-crack behaviours such as lower strength SFRC [108,109]. Khaloo and Kim [79], on the other hand, have discovered that the shear strength improvement from direct shear testing was more pronounced for higher strength concrete.

Furthermore, the combination of high-tensile strength fibres and low-strength concrete matrix tends to lead to pull-out at lower loads [4,110]. Accordingly, the mechanical anchorage cannot completely grow, resulting in low pull-out resistance [111]. The combination of steel fibres with lower tensile strength and high-strength concrete, on the other hand, are more likely to rupture early in the pull-out phase. To ensure the maximum mechanical anchorage contribution to the pull-out resistance, it is critical to provide a balanced combination of fibre and matrix strengths [112].

Several methods for increasing bond strength by improving the matrix consistency have been reported in the literature, including reducing the water/cement ratio [65,84,113], adding micro-fillers (e.g., fly ash and silica fume) [87,114,115], and using low-grade aggregates and high-strength cement [72]. With a reduction in the water/binder ratio from 0.45 to 0.29, the overall pull-out load was found to be improved by 30–40%, according to Jansson and Lofgren [67]. Robins and Austin [80] stated that adding 10% silica fume into the concrete mixture increased the pull-out load by about 50%. With a 30% increase in dose, the pull-out work increased almost twice as much. Shaikh and Shafaei [116] has discovered that adding 20% fly ash to the mix increased the overall pull-out load of hooked-end steel fibres by almost 50%.

Xu and Wu [117] found that the existence of coarse aggregates reduced the bond strength in general. This is due to the weakest connection in the fibre–matrix composites, where the coarse aggregates are contiguous to the interfacial region, de-bonding, and growing cracks. Furthermore, unlike the matrix's compressive power, the ultimate tensile strength of fibres has only a minor impact on the behaviour of SFRC. While a higher ultimate strength can improve a fibre's resistance to fracture, several studies have shown that fibre pull-out is the most common failure mode [5,118,119]. This is partly due to the high tensile strength of steel fibres, ranging from 1000 to 2300 MPa.

6. Experimental Research on the Strength and Bond Characteristics of SFRC

6.1. Compressive Strength

The compressive strength of concrete is one of the most important and commonly measured properties in various types and applications. Fibres must be used in order to prevent explosive failure and increase the ductility of concrete components. As compared to conventional concrete, the compressive behaviour of FRC with steel fibres is not significantly different. The key difference is that the compressive strength, ductility, and energy absorption are all enhanced. Their components determine the compressive strength of the composite materials, mix proportions, curing conditions, and fibre volume fractions and geometry [120]. Therefore, several studies have been conducted to examine the effects of steel fibres on the compressive strength of SFRC.

In this regard, Song and Hwang [121] have investigated the influence of steel fibres on the compressive strength of high-strength concrete (HSC) at different fibre volume fractions, ranging from 0.5 to 2.0% by volume of concrete. The highest compressive strength was achieved with the addition of 1.5% steel fibres, which were 15.3% higher than the plain HSC without fibres. According to a study by Ding and You [122], steel fibres had no noticeable effect on the compressive strength. They used hooked-end steel fibres with a length of 35 mm and a diameter of 0.55 mm at volume fractions of 25 and 50 kg/m³. The compressive strength of concrete was found to be almost similar to that of plain concrete. The quality and aspect ratio of fibres are key factors governing the compressive strength of concrete, as has been pointed out by Eren and Marar [123]. Steel fibres were used at higher dosages and aspect ratios in their analysis, which resulted in a higher increase in compressive strength. The impact of steel fibres on the compressive strength of SFRC mixtures comprising silica fume as a partial cement substitute has also been investigated by Köksal and Şahin [124], where silica fume was used at replacement levels of 5, 10, and 15% and steel fibres with aspect ratios of 65 and 80 were used at dosages of 0.5 and 1.0%. For the same silica fume and steel fibre content, compressive strength values of concrete mixtures with an aspect ratio of 80 were greater than those of mixtures with an aspect ratio of 65. As 1.0% steel fibres with aspect ratios of 80 and 65 were added to concrete mixtures, the compressive strengths of concrete specimens with 15% silica fume were increased by up to 117.6 and 113.8%, respectively, as compared to control specimens.

Furthermore, Shafaei and Shaikh [125] has investigated the impact of mineral admixtures and steel fibres on the performance of concrete. Silica fume and blast-furnace slag were used as partial cement replacements in their study, accounting for 10% and 20% by the weight of cement, respectively. A viable corrugated steel fibre with a length of 55 mm was

also used. The presence of steel fibres was found to impact the compressive strength of the concrete specimens substantially. The compressive strength of the mix with 20% slag was increased by around 30% after the addition of 2% steel fibres. Nili and Afroughsabet [73] have also studied the combined effect of silica fume and hooked-end steel fibres with a length of 60 mm on the compressive strength of concrete. The addition of silica fume and steel fibres considerably improved the compressive strength of concrete at all fibre volume fractions and curing periods. However, the improvement in strength was more significant under more extended curing periods, as attributed to the pozzolanic nature of silica fume. Another essential factor that determines the properties of concrete is the aspect ratio of fibres. The compressive strength of SFRC was increased by 4–19% after the steel fibres were added, according to Yazıcı and Arel [10]. Furthermore, SFRCs with 1.5, 1.0, and 0.5% fibre volume fractions had a maximum compressive strength for the aspect ratios of 45, 65, and 80, respectively.

The influence of the shape and geometry of steel fibres on the compressive strength of concrete has been investigated by Wu and Shi [89]. Steel fibres were applied in three different shapes (straight, corrugated, and hooked-end) to concrete mixtures in volume fractions of 1%, 2%, and 3%. Concrete mixtures containing hooked-end fibres had the highest compressive strengths, whereas those containing straight fibres had the lowest. At 28 days, the compressive strength of the control sample was recorded as 106.8 MPa. For 1%, 2%, and 3% of the straight steel fibres, the compressive strength increased by 21.95, 40.3, and 48%, respectively. The compressive strength increased by 33.7%, 48.7%, and 59.0% when the same volume fractions of hooked-end fibres were added, respectively. Consequently, it was proposed that hooked-end steel fibres outperform other-shaped steel fibres, in terms of mechanical efficiency, as has also been pointed out by Abdallah et al. [126].

6.2. Tensile Strength

Concrete's tensile strength is much lower than its compressive strength. This implies that cracks may spread rapidly under tensile loading, which causes brittle failure in unreinforced concrete specimens, as has been reported by Afroughbast et al. [127]. The concrete cover is likely to crack under load, even for reinforced concrete structural members, due to the poor tensile strength of concrete. Fibres can significantly improve the tensile behaviours of concrete composites, such as the durability, fracture toughness, and failure mode. Based on their overall tensile responses, fibre-reinforced concretes can be divided into strain-softening and strain-hardening. A low volume of short fibres is commonly used to strengthen strain-softening fibre-reinforced concrete. Zain et al. [128] have stated that concrete composites containing around 1% fibre are typically used in bulk field applications, such as those requiring large quantities of concrete. In the strain-softening type of failure, the concrete specimen only develops one key crack. Usually, a large amount of short fibres are used to strengthen strain-hardening fibre reinforced concrete. In continuous fibre-reinforced composites and short fibre-reinforced concrete, strain-hardening with several cracks has been observed. In addition, Li [129] has reported that the failure mode changes from strain-softening to strain-hardening. Additionally, Alhozaimy et al. [130] and Hsie et al. [131] have stated that the concrete tensile strength can be significantly increased by aligning fibres in the direction of tensile stress. However, the increase in strength for more or less uniformly dispersed fibres is much lower, ranging from no increase in some cases to around 60% higher than plain concrete.

Oluokun and Burdette [132] investigated the relationship between indirect tensile strength using cylindrical specimens and compressive strength in concrete with compressive strength up to 85 MPa after 28 days. It was shown that the indirect tensile strength can be as high as 10% of the compressive strength at low strengths but drops to 5% at higher strengths. The splitting tensile strength of crushed-rock aggregate concrete was around 8% higher than that of gravel aggregate concrete. Choi and Yuan [133] and Murali et al. [134] have studied the effects of steel fibres in concrete and found that incorporating steel fibres into the concrete components changed the failure mode. According to Lu and Hsu [135],

the HSC presented brittle shattering tensile failure when the lateral deformation exceeded its tensile potential, while the SFRC demonstrated more ductility without a sudden breakage of the cylinder, which may be attributed to the reinforcement effect of steel fibres. Sivakumar and Santhanam [136] have also found that adding steel fibres to concrete at very small doses (0.5%) resulted in a maximum increase in splitting tensile strength, ranging from 9 to 50% when compared to concrete without fibres.

Improvements in splitting the tensile strength have been observed for low contents (0.5–1%) and higher contents (1–2%) of fibres, ranging from 15 to 121% and from 40 to 143%, respectively. Song and Hwang [121] have reported that a 2% rise in the steel fibre volume fraction resulted in a 2% increase in the splitting tensile strength. The increase in the splitting tensile strength was estimated to range from 19 to 98.3%, depending on the type and shape of the steel fibres, compared to the control concrete. The addition of 2% steel fibres with a length of 32 mm to lightweight aggregate concrete can result in an increase in splitting tensile strength of up to 92.5%, as has been found by Wang and Wang [137]. The effect of the aspect ratio and fibre volume fractions on the splitting tensile strength of SFRC has been investigated by Yazıcı and İnan [138], where three aspect ratios (45, 65, and 80) were used, as well as three different fibre dosages (0.5, 1.0, and 1.5% by volume of concrete). Compared to the control mixture without any fibres, hooked-end bundled steel fibres led to an improvement in the splitting tensile strength values of SFRC, ranging from 11 to 54%.

The ability of fibres to restrain the expansion of cracks, decrease the degree of stress concentration at the tip of cracks, bridge macrocracks, and provide an anchoring mechanism (e.g., produced by their hooked ends) can explain these increases in splitting tensile strength. According to Abbass and Khan [139], increasing the aspect ratio and fibre dosages increased the splitting tensile strength of SFRC for different strengths of concrete as a factor of water/cement ratios. The use of 1.5% steel fibre was more successful in increasing the splitting tensile strength of concrete. Moreover, adding 1.5% hooked-end steel fibres to concrete improved the splitting tensile strength by about 159.8%, as has been reported by Sivakumar and Santhanam [136]. The tensile strength of concrete reinforced with 2% steel fibres and an aspect ratio of 60, which comprised 10% silica fume as partial cement replacement, was increased up to 129.9% [138]. In addition to enhancing the characteristics of the aggregate–paste interfacial zone, it has been discovered that silica fume improved the bonding between fibres and the cement matrix, leading to an improvement in concrete tensile strength [107].

6.3. Flexural Strength

The flexural strength and ductility of fibre-reinforced concrete can be sufficient for it to act as a structural component. Steel fibres have also been reported to more significantly impact the flexural strength than the compressive or tensile strength of concrete. The fibre volume fractions and aspect ratio of the fibres affect this increase in the flexural strength, with higher aspect ratios contributing to greater strength development [140,141]. This could be due to the interfacial bonds between the fibres and the matrix carrying the load that the concrete carried until cracking, after matrix cracking. According to Wang et al. [142], the fibres tend to mitigate sudden specimen failure and resist crack propagation, resulting in increased concrete load-carrying capability. The addition of up to 2% steel fibre increased the modulus of rupture (MOR), according to Song and Hwang [121], where the increase in MOR was estimated to range from 28.1 to 126.6%, depending on the fibre content, compared to plain concrete. The effects of fibre form, volume fraction, and length on the flexural behaviour of high-strength concrete have been investigated by Balaguru and Najm [143]. Compared to other forms of fibre, hooked-end steel fibres in concrete successfully raised its durability. It was also reported that fibre dosages in the 30–60 kg/m³ range were sufficient to achieve ductility. It was further discovered that corrugated and deformed-end fibres require a higher fibre volume fraction to achieve the same level of toughness. In the case of hooked-end steel fibres, the fibre length had no impact on the concrete's toughness.

Soroushian and Bayasi [144] have investigated the effect of different types of steel fibres on the flexural performance of high-performance concrete. Hooked-end steel fibres improved the energy absorption capacities and flexural strength greater than those in mixtures reinforced with straight and crimped steel fibres at aspect ratios of about 60 and 75 and with a given fibre volume fraction of 2%. The aspect ratio of steel fibre has a significant impact on the development of concrete flexural strength, according to Yazıcı and İnan [138]. The control concrete had a flexural strength of 5.94 MPa while, at 0.5, 1.0, and 1.5% fibre content, the minimum and maximum flexural strength values were 6.14, 6.24, and 6.42 MPa and 7.75, 9.33, and 10.76 MPa, respectively, for aspect ratios of 45, 65, and 80. Wu and Shi [89] investigated the effectiveness of steel fibres of various shapes in increasing the flexural strength of ultra-high-performance concrete (UHPC). The UHPC with hooked-end fibres had the greatest flexural strength, while the UHPC with straight fibres had the lowest. At 28 days, the reference UHPC sample had a flexural strength value of 19 MPa. When 1, 2, and 3% straight steel fibres were added, the flexural strength improved by 15.8, 42.1, and 89.5%, respectively. The flexural strength of specimens with hooked-end fibres was increased by 31, 73.7, and 121%, respectively, under the same fibre dosages. This may be due to the different bonding strengths associated with different fibre shapes. Chemical bonding, anchorage mechanical forces associated with fibre ends, and friction contribute to the bonding strength at the fibre–matrix interface. Compared to other shaped fibres, hooked-end fibres have been shown to have facilitate mechanical interlocking [78].

6.4. Pull-Out Behaviour of Steel Fibres

SFRC bond properties have been studied extensively in laboratories over the last few decades, considering both deformed and un-deformed fibres [76]. Several test approaches have been presented in order to directly or indirectly evaluate the shear strength of the interfacial bond between the fibre and cementitious matrix [11]. The pull-out test is one of the most specific ways to describe the interfacial properties between the fibre and matrix. This is an excellent test for simulating the practical case of fibres bridging cracks and obtaining a pull-out load versus slip relationship [77]. Pull-out tests have traditionally been used to examine the bond strength at the fibre–matrix interface [27,32]. These tests can be classified based on the technique used to apply the tensile stresses—for example, single- and double-sided tests—or the number of fibres embedded (i.e., single or multiple fibres). Considering its simplicity and configuration, one-sided pull-out tests have primarily been conducted on single fibres [102]. These tests have three key benefits for determining composite behaviour in operation: the geometry and design of the test sample are very close to those of single-fibre pull-out from a crack opening, residual stresses are caused in the sample due to matrix curing, and the interfacial bonding behaviour is exposed.

Many studies have been devoted to assessing the bond characteristics of steel fibre–matrix interfaces, especially using single fibre pull-out tests [101]. Numerous research results have been obtained with respect to influential variables, such as matrix intensity, fibre embedded length, fibre inclination angle, and temperature taken into account [75,80,125]. It has been well-established that, as fibre diameter, fibre-embedded weight, and matrix strength increase, so do pull-out load and toughness. In terms of the fibre shape effect, Torre-Casanova and Jason [112] indicated that hooked and deformed steel fibres provide greater pull-out resistance than those of straight steel, due to the mechanical interlocking contribution of the fibres. Furthermore, the chemical treatment of the fibre surface has been revealed to have a significant impact on the steel fibre–matrix interfacial bonding efficiency, mainly when mechanical interlocking is not present [11]. Others have looked into the effects of additives, curing conditions, and loading rate in ultra-high-performance concrete, in order to determine whether they affect the steel fibre–matrix interfacial properties [78].

Deng and Ding [11] investigated the interfacial bonding efficiency of steel fibres in steel–polypropylene hybrid fibre-reinforced cementitious composites. Single-sided pull-out tests were conducted to analyse two classes of straight and hooked-end steel fibre specimens in their sample, as depicted in Figure 9. The single-sided fibre pull-out test

specimen was a cubic concrete matrix with 100 mm diameter and a steel fibre inserted into the centre. The pull-out steel fibre was perpendicularly embedded after the concrete was cast into the mould for ease of use. The test setup used in their study is shown in Figure 10.

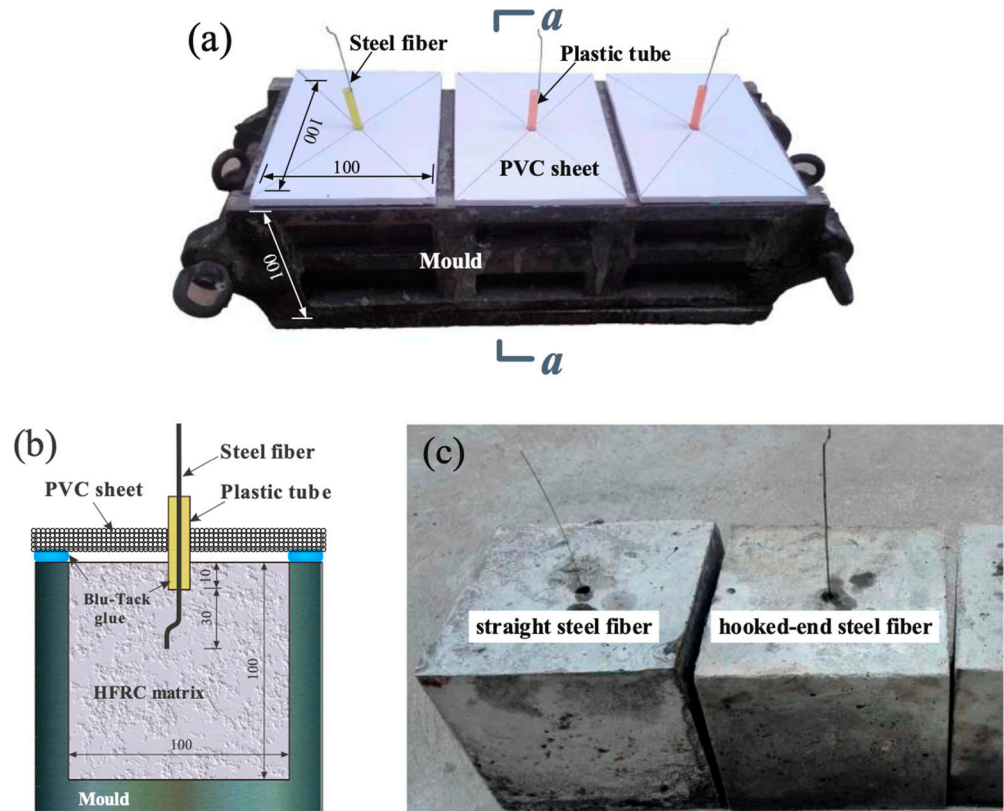


Figure 9. (a) Specimen casting in the moulds; (b) a–a cross-section; and (c) extracted pull-out specimens [11].

The standard responses for straight and hooked-end fibres are plotted in Figures 11 and 12, respectively, based on the fibre pull-out load vs. slip results. These pull-out processes can be broken down into several steps, each of which is denoted by a circle in the left curve. In the case of a straight steel fibre, there was an intact interface between the fibre and matrix in the first stage—referred to as the wholly bonded stage—and the resulting linear section of the pull-out load vs. slip curve only accounts for a small portion of the overall slippage. Some micro-cracks in the matrix near the fibre surface may develop at this point. The external force resistance, on the other hand, is dominated by chemical adhesion. At this point, the impact of fibres in the matrix is not apparent. Furthermore, the adhesion along the fibre–matrix interface was damaged partially in the second stage—referred to as de-bonding—as the pull-out force increased. The adhesive force in the residual intact zone acts in tandem with the frictional force in the de-bonded zone. When the bonded portion of the fibre becomes very short, the force reaches its peak. The inclusion of fibres in the matrix roughens the frictional surface, resulting in a greater pull-out load. Moreover, once the maximum force is reached in the third stage—referred to as frictional sliding—complete de-bonding occurs [126]. Consequently, the remaining segment’s pull-out force is solely due to the friction between the fibre and matrix. As the remaining fibre length in the matrix becomes shorter and shorter before the fibre is completely pulled out, the pull-out resistance gradually decreases to zero. The matrix fibres serve a similar purpose as the second-level fibres.

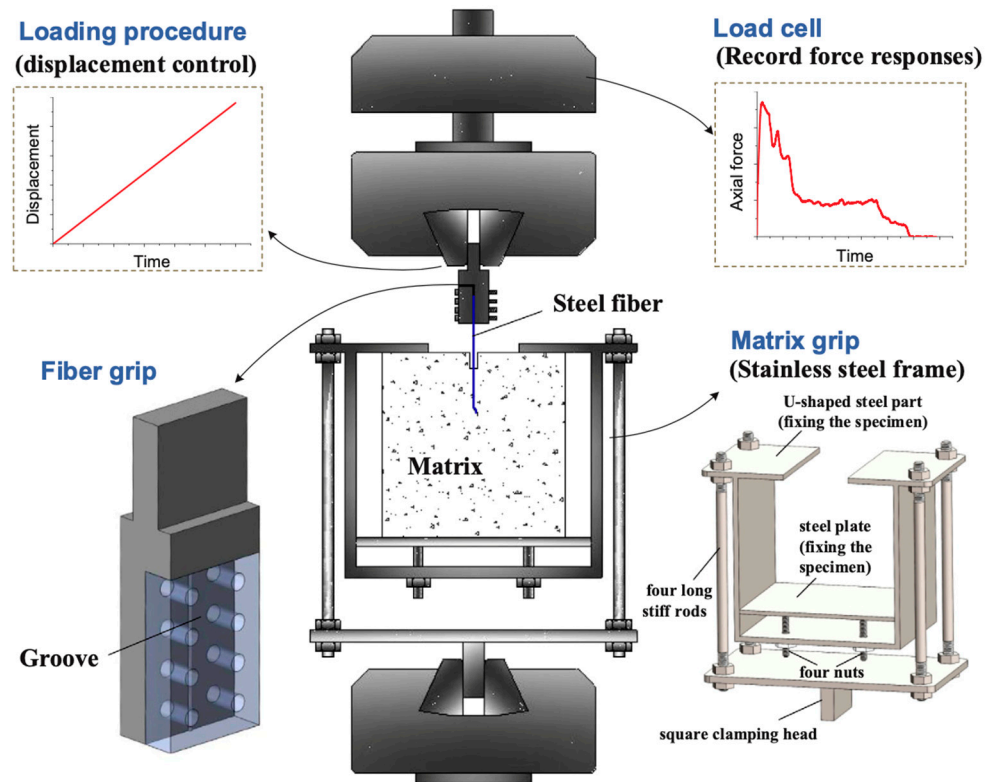


Figure 10. Pull-out test setup for a single fibre [11].

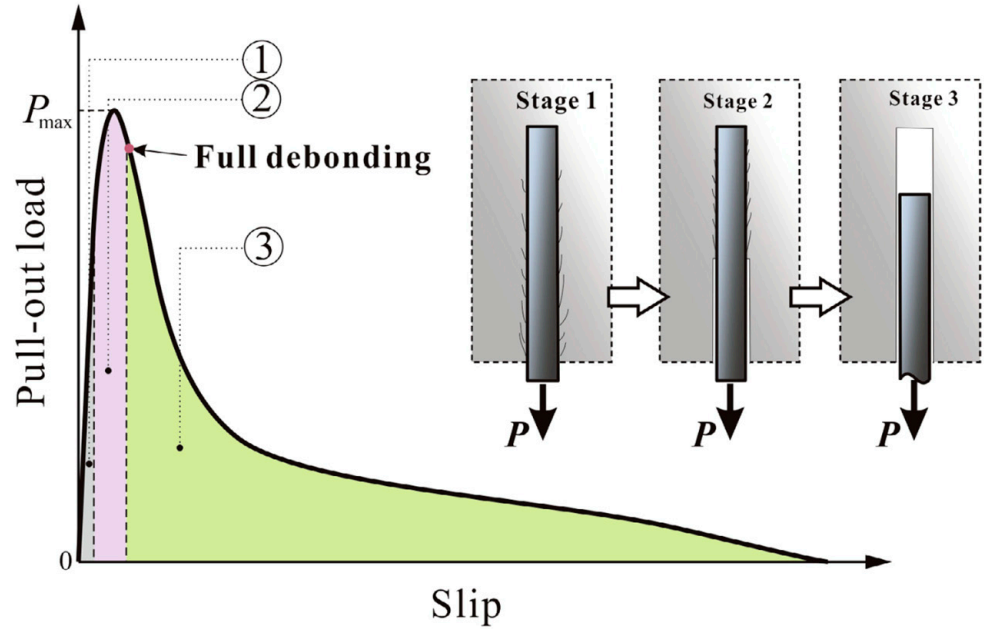


Figure 11. Pull-out behaviour of straight steel fibres embedded in concrete; these pull-out processes can be divided into several stages and each stage has been marked out with circles in left curves: Stage 1: fully bonded stage; Stage 2: debonding stage; Stage 3: frictional sliding stage [11].

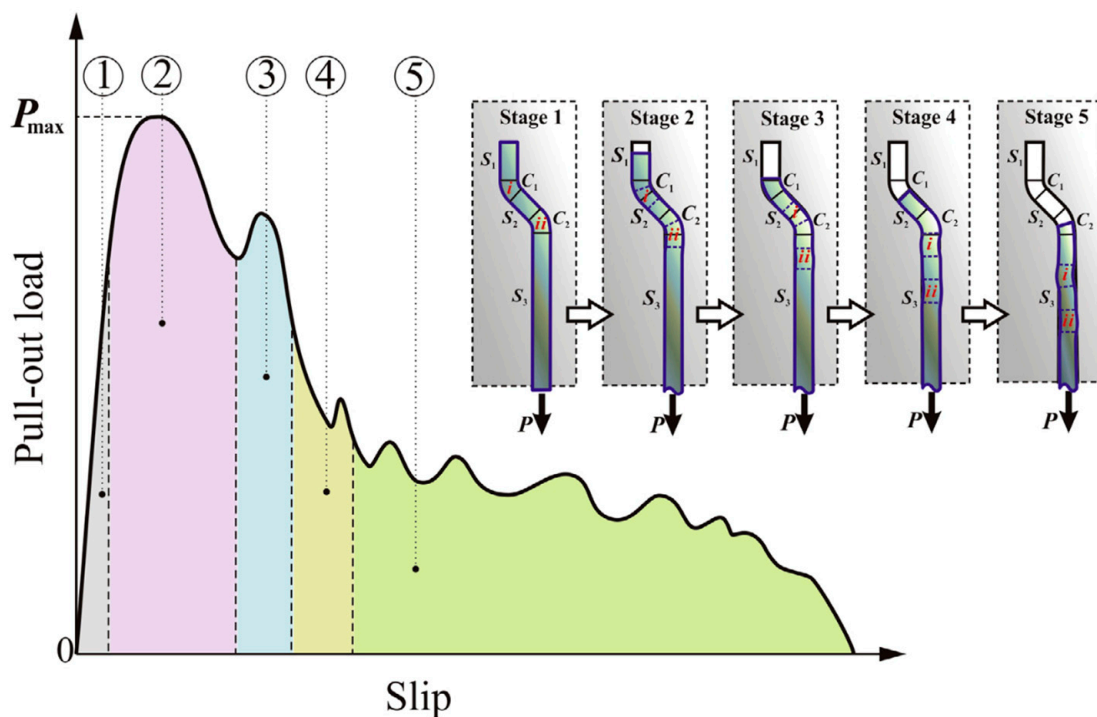


Figure 12. The pull-out performance of a hooked-end steel fibre embedded in concrete; these pull-out processes can be divided into several stages and each stage has been marked out with circles in left curves: Stage 1: elastic and partial debonding stage; Stage 2: the first plastic deformation stage; Stage 3: the second plastic deformation stage; Stage 4: deformation-sliding hybrid stage. Stage 5: frictional sliding stage [11].

In the case of hooked-end steel fibres, five different stages were identified, as shown in Figure 12. The first stage is known as partial and elastic de-bonding. This stage considers the elastic and partial de-bonding parts of the interface property until it fully de-bonds. Until the hooked-end fibre is totally de-bonded, the curve presents linear and non-linear components. The curved ducts of C1 and C2 align with the hook’s initial arc segments, as shown in Figure 12. This section compensates for the lowest part of the entire pull-out slip. In addition, after the fibre has been completely de-bonded, the curved segments i and ii begin to enter the straight ducts S2 and S3, and the fibre segments in the straight ducts S1 and S2 begin to enter the curved ducts in the second stage—also known as the first plastic deformation stage. Consequently, these fibre segments are increasingly exposed to bending and plastic deformation, increasing the pull-out load significantly. When the slippage is between 0.5 and 1.5 mm, the full pull-out load is often reached. At this point, the hybrid fibre effect is primarily manifested in two ways: resisting matrix cracking and increasing matrix power.

According to Abdallah and Fan [106], the remaining short fibre segment in S1 stiffens and the surrounding matrix deforms considerably. Accordingly, the concrete matrix with fibres has a greater supporting capacity, resulting in increased pull-out resistance. On the other hand, fibres aid in preventing micro-crack initiation and development, postponing the creation of macro-cracks near the hooked ends. After reaching its maximum value, the pull-out load drops to a specific value in stage 3—the second plastic deformation stage—before segment i enter the original print of segment ii, where it is forced to bend in the opposite direction to its original shape and the pull-out load reaches its second-highest point. At this phase, the fibre effect is similar to that at the previous level. At the fourth stage—a deformation-sliding hybrid stage—segment i moves into the straight duct S3, causing a mild decrease in pull-out load. The pull-out resistance is almost equally caused by friction along the duct S3 and decreasing plastic deformation. The frictional surface

becomes rougher as more fibres are added to the matrix, resulting in a greater force being applied to the fibre. Finally, after all the hooked sections have passed through the duct S3 in the fifth and frictional sliding phases, a residual resistance induced by the friction force can be detected, with no further plastic deformation of steel fibre. This residual force is also greater than that of straight fibres, due to the hook's incomplete straightening [23]. As the partially straightened fibre hook exits the straight duct S3 fully, the pull-out load rapidly decreases to zero.

In addition, Figure 13a depicts the impact of different fibre dosages on the maximum pull-out load P_{\max} of straight and hooked-end fibres in concrete mixtures. The maximum pull-out load reported was between 58 and 118 N for straight fibre specimens and between 311 and 403 N for hooked-end fibre samples. Furthermore, as the steel fibre content increases, the rising rate of the load decreases slightly. The P_{\max} appears to increase with the number of straight steel fibre specimens, as seen in Figure 13b, while the reinforcing effect of steel fibres appears to be less apparent in hooked-end steel fibre specimens. This is due to the lack of an impact of fibres reinforcing the mechanical interlocking, which controls the bond reaction of hooked-end fibres.

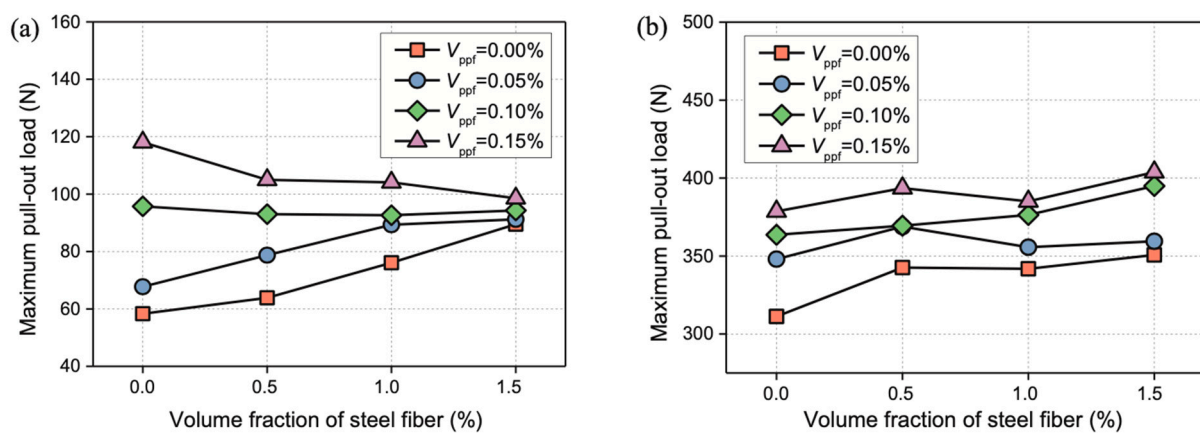


Figure 13. Effect of steel fibre dosage on maximum pull-out load (P_{\max}) for specimens including (a) straight fibres and (b) hooked-end fibres [11].

The spalling of specimens, rupture of fibres, and interface failure are the three types of failure modes commonly identified in fibre pull-out tests [145]. Deng and Ding [11] has indicated that all tests for straight steel fibres and hooked-end steel fibres ended with a pull-out failure mode for specimens with fibre-embedded lengths of 30 mm and 20 mm. The straight brass-coated fibres were extracted and the brass coating was scaled off on a clean surface. As shown in Figure 14a,b, the specimen failure mode for the hooked-end fibre with a fibre-embedded depth of 10 mm is controlled by both fibre pull-out and matrix spalling near the surface. After the test, it was discovered that the fibre could not be completely straightened and the hole remained in the matrix surface, which was widened from a circle to an ellipse. The inadequate matrix above the hook could no longer withstand the local pressure exerted by the fibre, resulting in matrix spalling (as shown in Figure 14c). Therefore, the fibre channel in the matrix was widened, causing it to be impossible to straighten the fibre. As shown in Figure 14d, when hybrid fibres are applied to the matrix, the channel expands less. This is due to the reinforcement effect of fibres on the crack resistance of concrete. Consequently, whether fibres are in the matrix or not, fibres embedded in the matrix that are too short are not suitable for completely exploiting the fibre–matrix interface bond property. To fully utilise the fibres with sufficient lengths, they must be embedded in a concrete matrix—particularly non-straight ones.

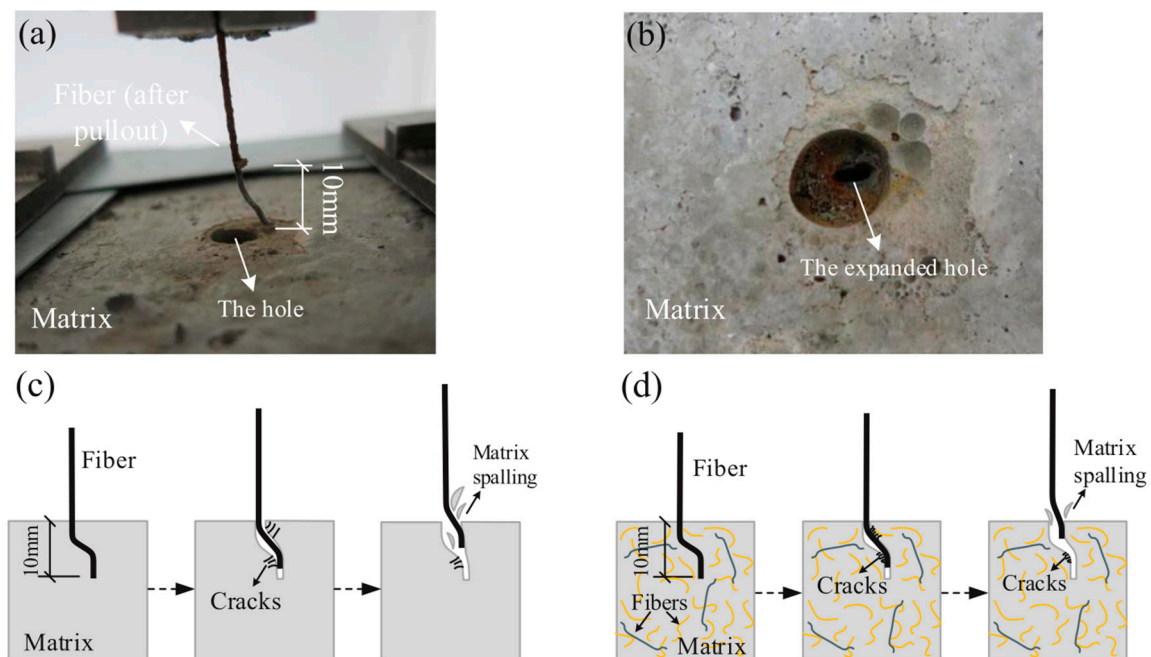


Figure 14. The modes of failure in pull-out test: (a) Matrix surface (b) after fibre pull-out; and fibre pull-out failure mechanism in the matrix (c) without and (d) with fibres [11].

In another study, Nieuwoudt and Boshoff [101] conducted pull-out tests on hooked-end and straight steel fibres using a similar method to Deng and Ding [11]. The straight fibre pull-out tests indicated that the pull-out load drops dramatically once the peak load is reached. This sudden decrease is caused by unstable de-bonding between the fibre and the matrix that surrounds it. After this de-bonding, the tension between the fibre and the matrix is the dominant mechanism of pull-out behaviour. The post-peak pull-out load decreases as the slip increases, due to a reduction in the friction region and the roughness of the matrix covering the fibre. As the mechanical anchorage of the fibre hook becomes available as the pull-out slip increases, the decrease in the post-peak load for hooked-end fibres is not as abrupt as it is for straight fibres, as shown in Figure 15. The pull-out behaviour occurred under frictional resistance when the hooked end is straightened, similar to the straight fibre experiments [146]. This phenomenon occurs at a slip of approximately 4.5 mm, corresponding to the straightened hook length. A distinct pull-out behaviour was observed during 2.5 mm/s, 0.025 mm/s, and 0.0025 mm/s hooked-end single fibre pull-out rate measurements, as shown in red in Figure 16. The hooked end did not fully straighten during the pull-out operation, resulting in distinct pull-out behaviour. Figure 16 shows the difference between a completely straightened and a partially straightened fibre. Furthermore, their results were close to those of Isla and Ruano [146], who studied the load–slip curves of concrete specimens reinforced with various steel fibres.

Tai and El-Tawil [26] have used an MTS high-rate servo-hydraulic testing system with an MTS Flex SE controller to perform single fibre pull-out experiments with different testing setups, as shown in Figure 17. A specially designed grip was used to hold the fibre connected to a force connection on the testing device. A grip was used to restrain the half dog-bone specimen used to test the regular ASTM tensile properties of concrete. In addition, three different types of fibres were used: aligned straight smooth (S), hooked (H), and twisted (T). To simulate a fibre being pulled out in a standard cracked tensile sample and minimize the elongation of the fibre's free length, the free length of the fibre was reduced throughout gripping. A laser sensor was used to calculate the slip at the reference point, defined in terms of the fibre end and matrix movement.

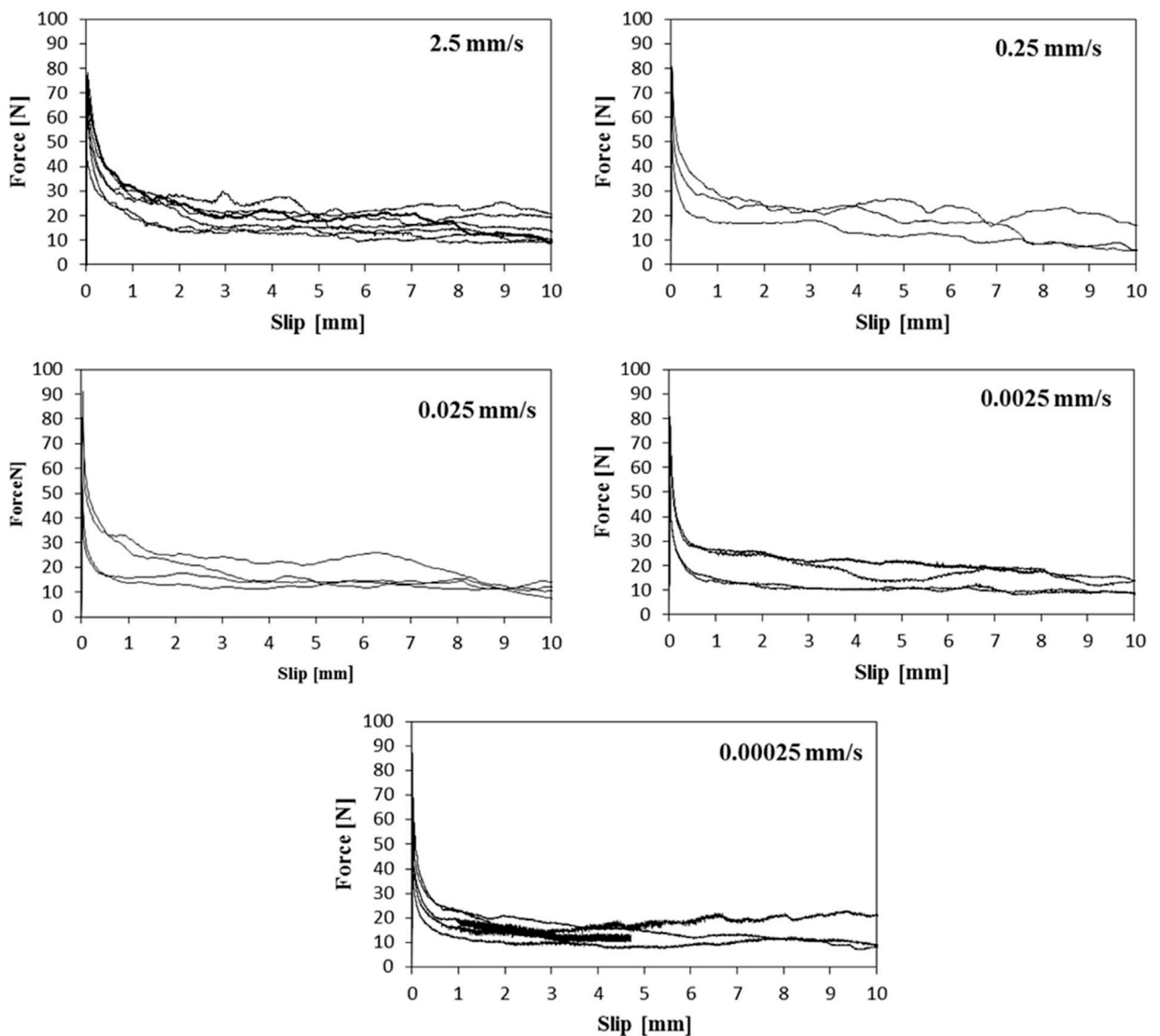


Figure 15. The single fibre pull-out test results on straight fibres [101].

Figures 18–20 depict the findings of their research. The results of the experiments for four different inclination angles with three loading rates on the pull-out load vs. slip curves of the S, H, and T specimens are presented. At least three specimens were used to average the curves for each pair. The pull-out behaviour of aligned S fibres differed from that of inclined S fibres, as shown in Figure 18. This may be directly due to the processes discussed previously. It is also evident, from Figure 18, that hardening arose at all the inclination angles and that the loading rate sensitivity is essential. However, in the H and T fibres, the effects of the loading rate and fibre inclination were not noticeable, as shown in Figure 19 and Figure 20, respectively. According to previous studies, the maximum pull-out load increases to an inclination angle of 30–45° before declining at 60° and beyond [27]. At a quasi-static loading rate (0.018 mm/s), the S fibres in their study adhered to this pattern, with the highest peak pull-out load (65.8 N) observed at a 45° inclination angle. The H and T fibres had slightly diverse patterns. At the inclination angles of 30° and 15°, the highest peak pull-out loads at the quasi-static loading rate were recorded as 229.2 N and 303.9 N, correspondingly. After the pull-out, the hooks of H fibres were straightened entirely and

spalling of the concrete matrix was observed at the exit point for H and T fibres, particularly with an increase in the inclination angle. The highest maximum pull-out loads for S fibres were 137.3 N and 135.9 N, respectively, at seismic and impact loading speeds, with both occurring at an inclination angle of 45°. The maximum values for H fibres were 245.5 N and 266.7 N, correspondingly, at 30° inclination. Under seismic and impact loading frequencies, the T fibre maximum peak loads were recorded as 274.9 N and 318.3 N, individually, at an inclination angle of 0°. It is unclear why the aligned T fibres presented a higher load capacity than inclined T fibres, compared to the other fibre varieties. The geometric shape of T fibres and their larger thickness are thought to have led to a higher spalling rate of the matrix at the exit point, lowering the total pull-out strength.

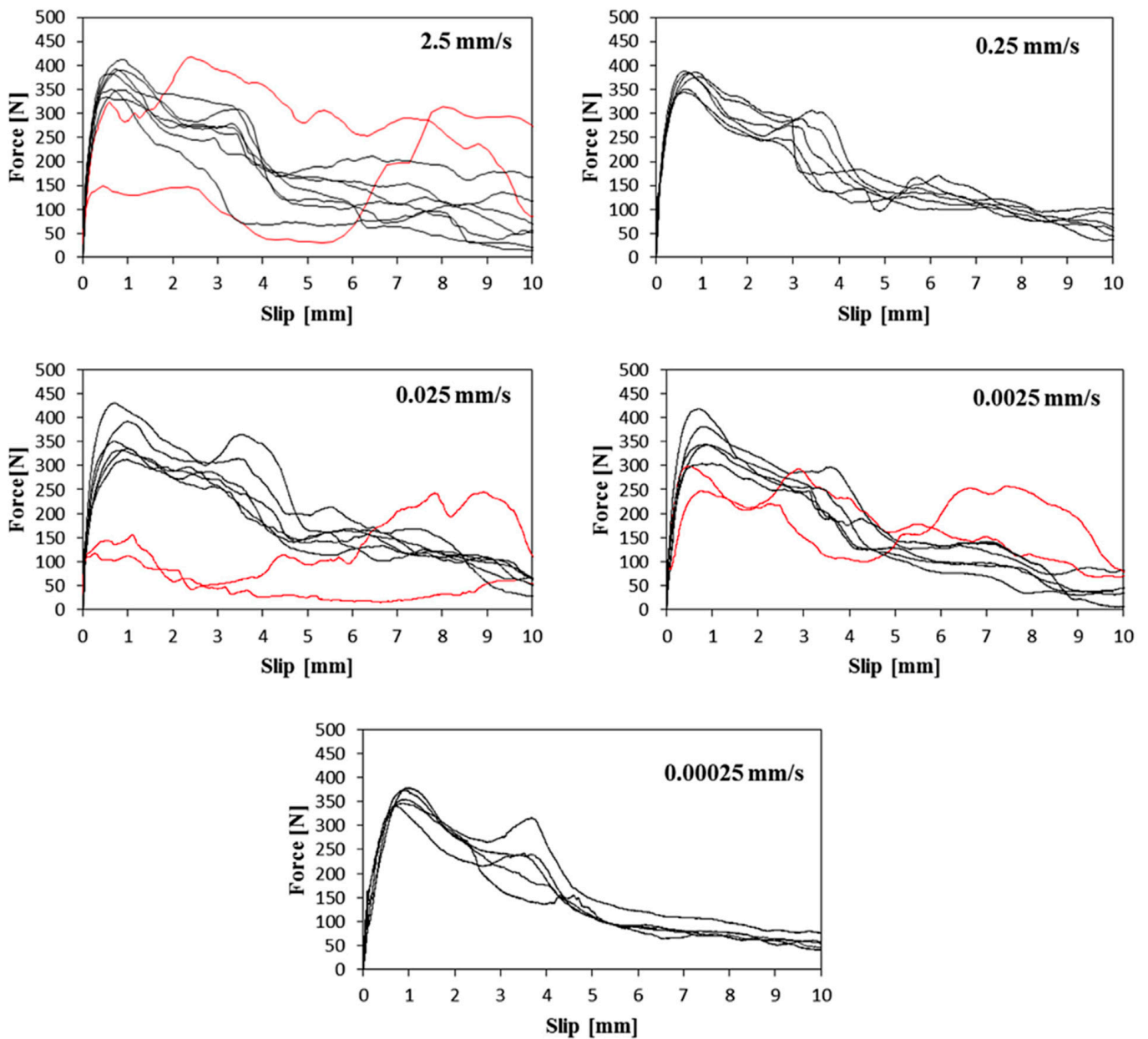


Figure 16. The single fibre pull-out test results on hooked-end fibres [101].

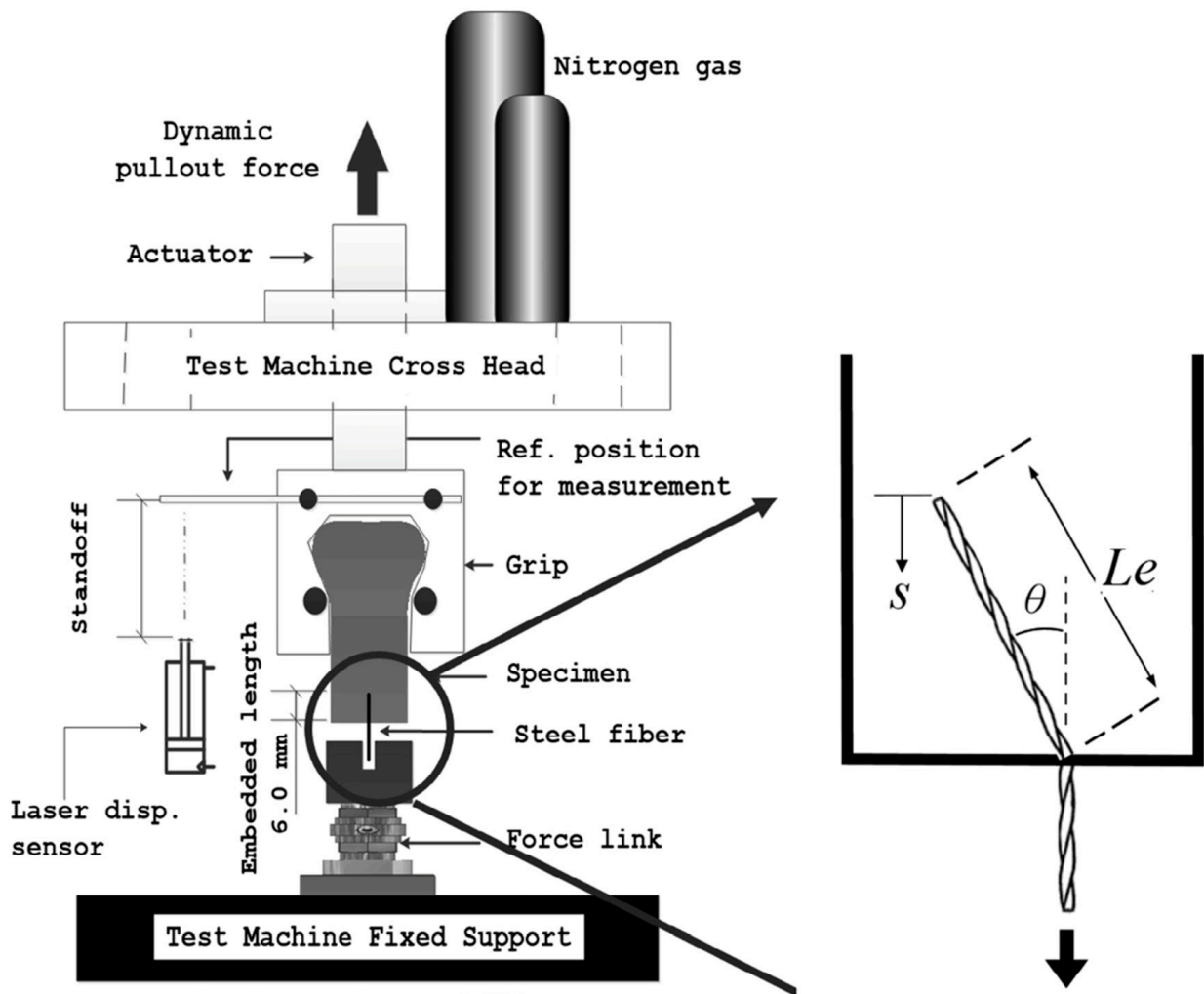


Figure 17. Schematic of inclined steel fibre pull-out test setup [26].

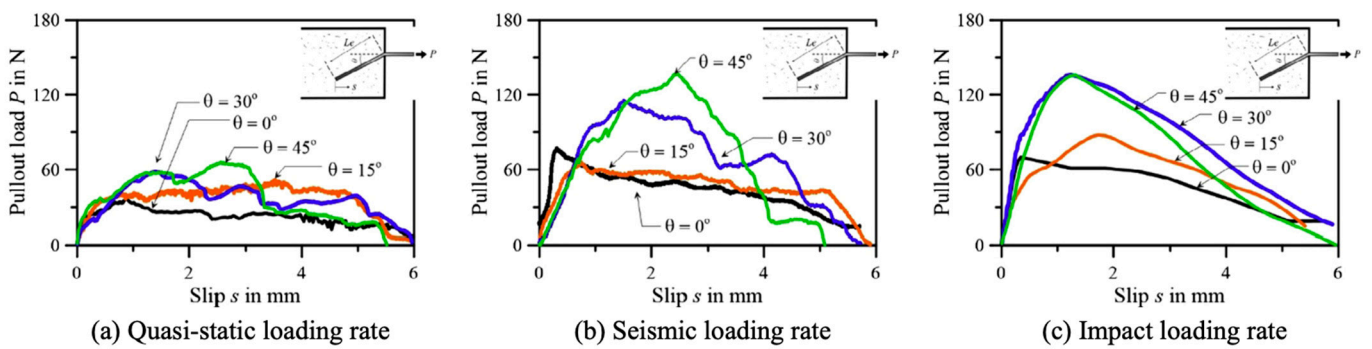


Figure 18. Average pull-out load vs. slip curves for S fibres embedded in UHPC under several loading rates and inclination angles: (a) quasi-static loading rate; (b) seismic loading rate; and (c) impact loading rate [26].

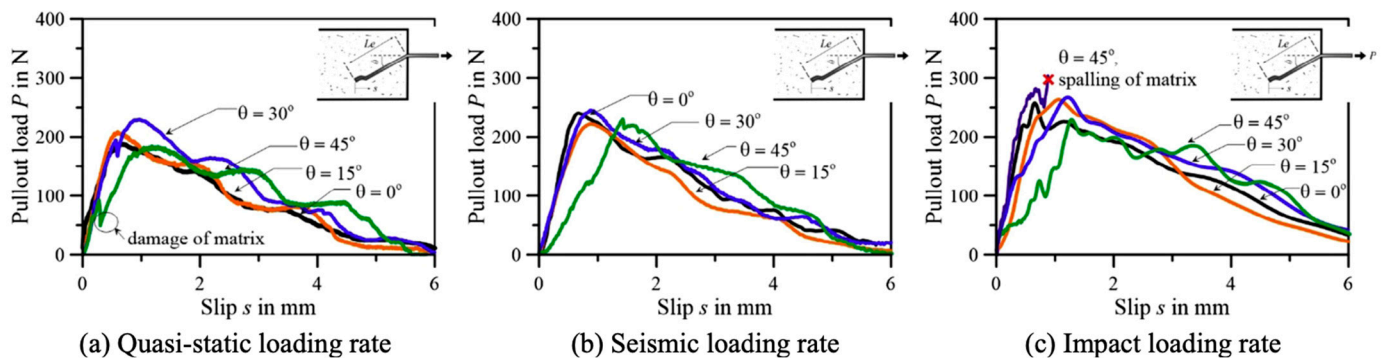


Figure 19. Average pull-out load vs. slip curves for H fibres embedded in UHPC under different loading rates and inclination angles: (a) quasi-static loading rate; (b) seismic loading rate; and (c) impact loading rate [26].

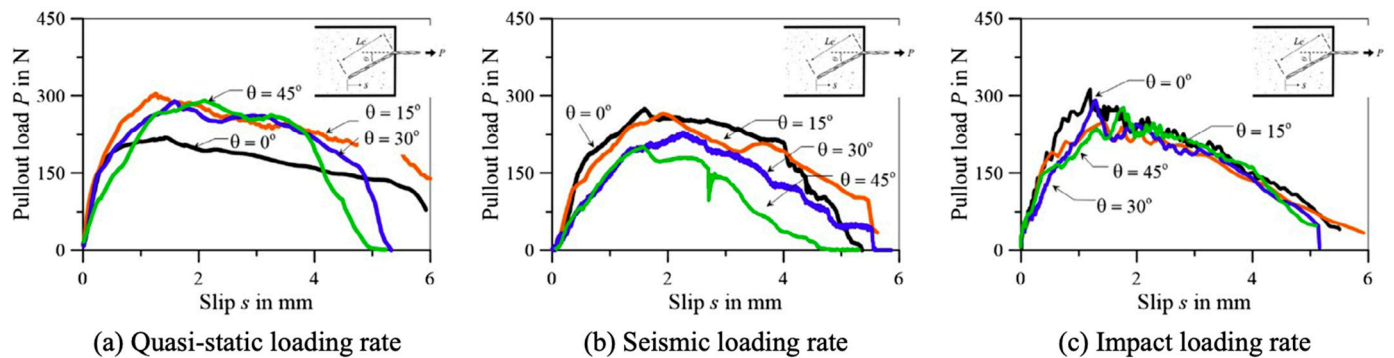


Figure 20. Average pull-out load vs. slip curves for T fibres embedded in UHPC matrix under different loading rates and inclination angles: (a) quasi-static loading rate; (b) seismic loading rate; and (c) impact loading rate [26].

7. Conclusions and Future Perspectives

Steel fibre-reinforced concrete (SFRC) has been shown to be a durable construction material and it is increasingly likely that it will be used in an extensive range of applications in the near future. The bonding between the reinforcing fibres and the concrete matrix is critical for ensuring adequate performance of the composite material. However, the bond behaviour of SFRC is still not yet fully understood. This research offers a thorough and in-depth evaluation of the bonding mechanisms underpinning the pull-out behaviour of steel fibres of several geometries and at various matrix strengths. We covered significant factors influencing the bond behaviour of SFRC at two different scales: single fibre pull-out and steel bar pull-out. Many physical factors, including geometry, diameter, embedded length, volume fraction, fibre alignment, and matrix quality, as well as their effects on the fresh and hardened properties of SFRC and pull-out behaviour, were examined. A comprehensive literature review was conducted, in order to enhance understanding of the bond performance of SFRC. The following conclusions can be drawn from the findings of this review:

1. The addition of fibres, especially steel fibres, increases the compressive strength of SFRC in general; however, the inclusion of more than 2% steel fibre is expected to result in a decrease in strength, due to decreased workability and higher pore content.
2. Steel fibres have a much greater impact on improving the splitting tensile strength and flexural strength than on improving compressive strength. The strength increases as the fibre aspect ratio rises at a given fibre content. The tensile and flexural strengths of concrete containing 2.0% steel fibre have been found to be increased by up to 143 and 167%, respectively.

3. The hook geometry of the fibre had a significant impact on its mechanical anchorage efficacy. The pull-out behaviour is directly influenced by the number of bends at the fibre ends. Even though all hooked-end fibres had the same diameter and embedded weight, there was a significant difference in their pull-out performance under hook geometry variations.
4. Compared to chemical adhesion, the sliding frictional force of straight steel fibre is less susceptible to fibre addition. The addition of hybrid fibres affects mechanical hook interlocking and controls the maximum pull-out load.
5. The bonding mechanisms that control the pull-out performance of inclined fibres are very different from those that control the pull-out behaviour of aligned fibres. The maximum pull-out load and pull-out feature of inclined fibres are higher than those of aligned fibres, up to a 15° inclination angle. Nevertheless, as the inclination angle increases to 45° and beyond, the pull-out load decreases due to fibre bending and matrix spalling and all the hooked-end fibres may be ruptured.
6. The loads required to pull out the deformed steel bars embedded in the specimens prepared from concretes are related to the mechanical properties of the concrete, the cover, steel fibre dosage, and the steel fibre aspect ratio.

Pull-out experiments are also commonly used to study bond properties at the fibre–matrix interface. Despite this, there is no universally accepted formula for assessing the bond strength in SFRC. Several papers have attempted to develop bond-slip characteristics using the most effective process of pre-deforming fibre. However, there have been few attempts to optimise fibre size and shape in this field. Furthermore, the effect of fibre orientation on pull-out behaviour is still unknown. While both straight and hooked-end fibres embedded in concrete composites have similar pull-out responses at different inclination angles, the bonding mechanisms of hooked-end fibres are expected to differ, depending on the matrix strength. As such, more studies—both experimentally and using finite element modelling—are needed to fully understand the effect of matrix strength on the pull-out behaviour of inclined fibres.

Author Contributions: Conceptualization, M.A.M. and S.D.; methodology, M.A.M., S.D. and E.M.; validation, S.D., E.M. and A.H.; investigation, M.A.M. and A.M.; resources, M.A.M. and S.D.; writing—original draft preparation, M.A.M.; writing—review and editing, M.A.M., S.D., A.H. and A.M.; visualization, M.A.M., S.D., E.M., A.H. and A.M.; supervision, S.D.; project administration, M.A.M., S.D., E.M., A.H. and A.M. All authors have read and agreed to the published version of the manuscript.

Funding: This research received no external funding.

Acknowledgments: This publication was supported by the Deanship of Scientific Research at Prince Sattam bin Abdulaziz University, Alkharj, Saudi Arabia.

Conflicts of Interest: The authors declare no conflict of interest.

References

1. Zollo, R.F. Fiber-reinforced concrete: An overview after 30 years of development. *Cem. Concr. Compos.* **1997**, *19*, 107–122. [[CrossRef](#)]
2. Abdulhameed, A.A.; Al-Zuhairi, A.H.; Al Zaidee, S.R.; Hanoon, A.N.; Al Zand, A.W.; Hason, M.M.; Abdulhameed, H.A. The Behavior of Hybrid Fiber-Reinforced Concrete Elements: A New Stress-Strain Model Using an Evolutionary Approach. *Appl. Sci.* **2022**, *12*, 2245. [[CrossRef](#)]
3. Brandt, A.M. Fibre reinforced cement-based (FRC) composites after over 40 years of development in building and civil engineering. *Compos. Struct.* **2008**, *86*, 3–9. [[CrossRef](#)]
4. Abdulhameed, A.A.; Said, A.I. CFRP laminates reinforcing performance of short-span wedge-blocks segmental beams. *Fibers* **2020**, *8*, 6. [[CrossRef](#)]
5. Abdulhameed, A.A.; Hanoon, A.N.; Abdulhameed, H.A.; Banyhussan, Q.S.; Mansi, A.S. Push-out test of steel–concrete–steel composite sections with various core materials: Behavioural study. *Arch. Civ. Mech. Eng.* **2021**, *21*, 17. [[CrossRef](#)]

6. García-Taengua, E.; Martí-Vargas, J.R.; Serna, P. Bond of rebars to steel fibre reinforced concrete: Minimum concrete cover requirements to prevent splitting. In *Concrete-Innovation and Design*; International Federation for Structural Concrete (fib): Lausanne, Switzerland, 2015.
7. Mohammadhosseini, H.; Yatim, J.M.; Sam, A.R.M.; Awal, A.A. Durability performance of green concrete composites containing waste carpet fibers and palm oil fuel ash. *J. Clean. Prod.* **2017**, *144*, 448–458. [[CrossRef](#)]
8. Rossi, P.; Charron, J.P.; Bastien-Masse, M.; Tailhan, J.L.; Le Maou, F.; Ramanich, S. Tensile basic creep versus compressive basic creep at early ages: Comparison between normal strength concrete and a very high strength fibre reinforced concrete. *Mater. Struct.* **2014**, *47*, 1773–1785. [[CrossRef](#)]
9. Garcia-Taengua, E.; Marti-Vargas, J.R.; Serna-Ros, P. Statistical Approach to Effect of Factors Involved in Bond Performance of Steel Fiber-Reinforced Concrete. *Aci Struct. J.* **2011**, *108*, 461–468.
10. Yazıcı, Ş.; Arel, H.Ş. The effect of steel fiber on the bond between concrete and deformed steel bar in SFRCs. *Constr. Build. Mater.* **2013**, *40*, 299–305. [[CrossRef](#)]
11. Deng, F.; Ding, X.; Chi, Y.; Xu, L.; Wang, L. The pull-out behavior of straight and hooked-end steel fiber from hybrid fiber reinforced cementitious composite: Experimental study and analytical modelling. *Compos. Struct.* **2018**, *206*, 693–712. [[CrossRef](#)]
12. Zile, E.; Zile, O. Effect of the fiber geometry on the pullout response of mechanically deformed steel fibers. *Cem. Concr. Res.* **2013**, *44*, 18–24. [[CrossRef](#)]
13. Frazão, C.; Barros, J.; Camões, A.; Alves, A.C.; Rocha, L. Corrosion effects on pullout behavior of hooked steel fibers in self-compacting concrete. *Cem. Concr. Res.* **2016**, *79*, 112–122. [[CrossRef](#)]
14. Yoo, D.-Y.; Je, J.; Choi, H.-J.; Sukontasukkul, P. Influence of embedment length on the pullout behavior of steel fibers from ultra-high-performance concrete. *Mater. Lett.* **2020**, *276*, 128233. [[CrossRef](#)]
15. Feng, J.; Sun, W.; Wang, X.; Shi, X. Mechanical analyses of hooked fiber pullout performance in ultra-high-performance concrete. *Constr. Build. Mater.* **2014**, *69*, 403–410. [[CrossRef](#)]
16. Qi, J.; Wu, Z.; Ma, Z.J.; Wang, J. Pullout behavior of straight and hooked-end steel fibers in UHPC matrix with various embedded angles. *Constr. Build. Mater.* **2018**, *191*, 764–774. [[CrossRef](#)]
17. Yoo, D.-Y.; Choi, H.-J.; Kim, S. Bond-slip response of novel half-hooked steel fibers in ultra-high-performance concrete. *Constr. Build. Mater.* **2019**, *224*, 743–761. [[CrossRef](#)]
18. Soulioti, D.; Barkoula, N.-M.; Koutsianopoulos, F.; Charalambakis, N.; Matikas, T. The effect of fibre chemical treatment on the steel fibre/cementitious matrix interface. *Constr. Build. Mater.* **2013**, *40*, 77–83. [[CrossRef](#)]
19. Zhang, H.; Ji, T.; Lin, X. Pullout behavior of steel fibers with different shapes from ultra-high performance concrete (UHPC) prepared with granite powder under different curing conditions. *Constr. Build. Mater.* **2019**, *211*, 688–702. [[CrossRef](#)]
20. Li, L.; Li, B.; Wang, Z.; Zhang, Z.; Alselwi, O. Effects of Hybrid PVA–Steel Fibers on the Mechanical Performance of High-Ductility Cementitious Composites. *Buildings* **2022**, *12*, 1934. [[CrossRef](#)]
21. Kim, B.-J.; Yi, C.; Ahn, Y.-R. Effect of embedment length on pullout behavior of amorphous steel fiber in Portland cement composites. *Constr. Build. Mater.* **2017**, *143*, 83–91. [[CrossRef](#)]
22. Yoo, D.-Y.; Park, J.-J.; Kim, S.-W. Fiber pullout behavior of HPRFCC: Effects of matrix strength and fiber type. *Compos. Struct.* **2017**, *174*, 263–276. [[CrossRef](#)]
23. Cao, Y.Y.Y.; Yu, Q.L. Effect of inclination angle on hooked end steel fiber pullout behavior in ultra-high performance concrete. *Compos. Struct.* **2018**, *201*, 151–160. [[CrossRef](#)]
24. Yoo, D.-Y.; Kim, J.-J.; Chun, B. Dynamic pullout behavior of half-hooked and twisted steel fibers in ultra-high-performance concrete containing expansive agents. *Composites. Part B Eng.* **2019**, *167*, 517–532. [[CrossRef](#)]
25. Lee, J.-H.; Kighuta, K. Twin-twist effect of fibers on the pullout resistance in cementitious materials. *Constr. Build. Mater.* **2017**, *146*, 555–562. [[CrossRef](#)]
26. Tai, Y.-S.; El-Tawil, S. High loading-rate pullout behavior of inclined deformed steel fibers embedded in ultra-high performance concrete. *Constr. Build. Mater.* **2017**, *148*, 204–218. [[CrossRef](#)]
27. Awal, A.A.; Mohammadhosseini, H. Green concrete production incorporating waste carpet fiber and palm oil fuel ash. *J. Clean. Prod.* **2016**, *137*, 157–166. [[CrossRef](#)]
28. Kim, J.J.; Yoo, D.Y. Spacing and bundling effects on rate-dependent pullout behavior of various steel fibers embedded in ultra-high-performance concrete. *Arch. Civ. Mech. Eng.* **2020**, *20*, 46. [[CrossRef](#)]
29. Yoo, D.-Y.; Kim, S.; Kim, J.-J.; Chun, B. An experimental study on pullout and tensile behavior of ultra-high-performance concrete reinforced with various steel fibers. *Constr. Build. Mater.* **2019**, *206*, 46–61. [[CrossRef](#)]
30. Cunha, V.M.C.F.; Barros, J.A.O.; Sena-Cruz, J.M. An integrated approach for modelling the tensile behaviour of steel fibre reinforced self-compacting concrete. *Cem. Concr. Res.* **2011**, *41*, 64–76. [[CrossRef](#)]
31. Aslani, F.; Nejadi, S. Bond characteristics of steel fiber and deformed reinforcing steel bar embedded in steel fiber reinforced self-compacting concrete (SFRSCC). *Open Eng.* **2012**, *2*, 445–470. [[CrossRef](#)]
32. Abdallah, S.; Fan, M.; Cashell, K.A. Bond-slip behaviour of steel fibres in concrete after exposure to elevated temperatures. *Constr. Build. Mater.* **2017**, *140*, 542–551. [[CrossRef](#)]
33. Zhang, Y.; Ju, J.W.; Chen, Q.; Yan, Z.; Zhu, H.; Jiang, Z. Characterizing and analyzing the residual interfacial behavior of steel fibers embedded into cement-based matrices after exposure to high temperatures. *Compos. Part B Eng.* **2020**, *191*, 107933. [[CrossRef](#)]

34. Mohammadhosseini, H.; Alyousef, R.; Poi Ngian, S.; Tahir, M.M. Performance evaluation of sustainable concrete comprising waste polypropylene food tray fibers and palm oil fuel ash exposed to sulfate and acid attacks. *Crystals* **2021**, *11*, 966. [[CrossRef](#)]
35. Chun, B.; Yoo, D.-Y. Hybrid effect of macro and micro steel fibers on the pullout and tensile behaviors of ultra-high-performance concrete. *Compos. Part B Eng.* **2019**, *162*, 344–360. [[CrossRef](#)]
36. Luccioni, B.; Ruano, G.; Isla, F.; Zerbino, R.; Giaccio, G. A simple approach to model SFRC. *Constr. Build. Mater.* **2012**, *37*, 111–124. [[CrossRef](#)]
37. Mohammadhosseini, H.; Alrshoudi, F.; Tahir, M.M.; Alyousef, R.; Alghamdi, H.; Alharbi, Y.R.; Alsaif, A. Durability and thermal properties of prepacked aggregate concrete reinforced with waste polypropylene fibers. *J. Build. Eng.* **2020**, *32*, 101723. [[CrossRef](#)]
38. Gandomi, A.; Alavi, A.; Yun, G. Nonlinear modeling of shear strength of SFRC beams using linear genetic programming. *Struct. Eng. Mech.* **2011**, *38*, 1–25. [[CrossRef](#)]
39. Zhang, W.; Lee, D.; Lee, C.; Zhang, X.; Ikechukwu, O. Bond performance of SFRC considering random distributions of aggregates and steel fibers. *Constr. Build. Mater.* **2021**, *291*, 123304. [[CrossRef](#)]
40. Abdallah, S.; Fan, M.; Rees, D.W.A. Bonding Mechanisms and Strength of Steel Fiber-Reinforced Cementitious Composites: Overview. *J. Mater. Civ. Eng.* **2018**, *30*, 04018001. [[CrossRef](#)]
41. Zhou, A.; Yu, Z.; Wei, H.; Tam, L.H.; Liu, T.; Zou, D. Understanding the Toughening Mechanism of Silane Coupling Agents in the Interfacial Bonding in Steel Fiber-Reinforced Cementitious Composites. *ACS Appl. Mater. Interface* **2020**, *12*, 44163–44171. [[CrossRef](#)]
42. Bandelt, M.J.; Frank, T.E.; Lepech, M.D.; Billington, S.L. Bond behavior and interface modeling of reinforced high-performance fiber-reinforced cementitious composites. *Cem. Concr. Compos.* **2017**, *83*, 188–201. [[CrossRef](#)]
43. Yoo, D.-Y.; Gim, J.Y.; Chun, B. Effects of rust layer and corrosion degree on the pullout behavior of steel fibers from ultra-high-performance concrete. *J. Mater. Res. Technol.* **2020**, *9*, 3632–3648. [[CrossRef](#)]
44. Naaman, A.E.; Namur, G.G.; Alwan, J.M.; Najm, H.S. Fiber Pullout and Bond Slip. II: Experimental Validation. *J. Struct. Eng.* **1991**, *117*, 2791–2800. [[CrossRef](#)]
45. Naaman, A.E.; Namur, G.G.; Alwan, J.M.; Najm, H.S. Fiber Pullout and Bond Slip. I: Analytical Study. *J. Struct. Eng.* **1991**, *117*, 2769–2790. [[CrossRef](#)]
46. Wang, X.H.; Jacobsen, S.; He, J.Y.; Zhang, Z.L.; Lee, S.F.; Lein, H.L. Application of nanoindentation testing to study of the interfacial transition zone in steel fiber reinforced mortar. *Cem. Concr. Res.* **2009**, *39*, 701–715. [[CrossRef](#)]
47. Su, Y.; Li, J.; Wu, C.; Wu, P.; Tao, M.; Li, X. Mesoscale study of steel fibre-reinforced ultra-high performance concrete under static and dynamic loads. *Mater. Des.* **2017**, *116*, 340–351. [[CrossRef](#)]
48. Allison, P.; Weiss, C.; Moser, R.; Diaz, A.; Rivera, O.; Holton, S. Nanoindentation and SEM/EDX characterization of the geopolymer-to-steel interfacial transition zone for a reactive porcelain enamel coating. *Compos. Part B Eng.* **2015**, *78*, 131–137. [[CrossRef](#)]
49. Xu, L.; Deng, F.; Chi, Y. Nano-mechanical behavior of the interfacial transition zone between steel-polypropylene fiber and cement paste. *Constr. Build. Mater.* **2017**, *145*, 619–638. [[CrossRef](#)]
50. Zacharda, V.; Němeček, J.; Štemberk, P. Nanomechanical Performance of Interfacial Transition Zone in Fiber Reinforced Cement Matrix. *Key Eng. Mater.* **2018**, *760*, 251–256. [[CrossRef](#)]
51. Zacharda, V.; Němeček, J.; Štemberk, P. Micromechanical performance of interfacial transition zone in fiber-reinforced cement matrix. *IOP Conf. Ser. Mater. Sci. Eng.* **2017**, *246*, 12018. [[CrossRef](#)]
52. Feng, H.; Li, L.; Zhang, P.; Gao, D.; Zhao, J.; Feng, L.; Sheikh, M.N. Microscopic characteristics of interface transition zone between magnesium phosphate cement and steel fiber. *Constr. Build. Mater.* **2020**, *253*, 119179. [[CrossRef](#)]
53. Teixeira, R.; Tonoli, G.; Santos, S.; Rayón, E.; Amigó, V.; Savastano, H.; Lahr, F.R. Nanoindentation study of the interfacial zone between cellulose fiber and cement matrix in extruded composites. *Cem. Concr. Compos.* **2018**, *85*, 1–8. [[CrossRef](#)]
54. Liu, J.; Farzadnia, N.; Shi, C. Effects of superabsorbent polymer on interfacial transition zone and mechanical properties of ultra-high performance concrete. *Constr. Build. Mater.* **2020**, *231*, 117142. [[CrossRef](#)]
55. Kang, S.H.; Kim, J.J.; Kim, D.J.; Chung, Y.-S. Effect of sand grain size and sand-to-cement ratio on the interfacial bond strength of steel fibers embedded in mortars. *Constr. Build. Mater.* **2013**, *47*, 1421–1430. [[CrossRef](#)]
56. Wu, Z.; Shi, C.; Khayat, K.H. Influence of silica fume content on microstructure development and bond to steel fiber in ultra-high strength cement-based materials (UHSC). *Cem. Concr. Compos.* **2016**, *71*, 97–109. [[CrossRef](#)]
57. Rossignolo, J.A.; Rodrigues, M.S.; Frias, M.; Santos, S.F.; Junior, H.S. Improved interfacial transition zone between aggregate-cementitious matrix by addition sugarcane industrial ash. *Cem. Concr. Compos.* **2017**, *80*, 157–167. [[CrossRef](#)]
58. Zhang, L.; Zhang, Y.; Liu, C.; Liu, L.; Tang, K. Study on microstructure and bond strength of interfacial transition zone between cement paste and high-performance lightweight aggregates prepared from ferrochromium slag. *Constr. Build. Mater.* **2017**, *142*, 31–41. [[CrossRef](#)]
59. Erdem, S.; Dawson, A.R.; Thom, N.H. Influence of the micro- and nanoscale local mechanical properties of the interfacial transition zone on impact behavior of concrete made with different aggregates. *Cem. Concr. Res.* **2012**, *42*, 447–458. [[CrossRef](#)]
60. Mondai, P.; Shah, S.R.; Marks, L.D. Nanoscale characterization of cementitious materials. *ACI Mater. J.* **2008**, *105*, 174–179.
61. Valcuende, M.; Parra, C. Bond behaviour of reinforcement in self-compacting concretes. *Constr. Build. Mater.* **2009**, *23*, 162–170. [[CrossRef](#)]

62. Sharaky, I.; Torres, L.; Baena, M.; Miàs, C. An experimental study of different factors affecting the bond of NSM FRP bars in concrete. *Compos. Struct.* **2013**, *99*, 350–365. [[CrossRef](#)]
63. Berrocal, C.G.; Fernandez, I.; Lundgren, K.; Lofgren, I. Corrosion-induced cracking and bond behaviour of corroded reinforcement bars in SFRC. *Composites. Part B Eng.* **2017**, *113*, 123–137. [[CrossRef](#)]
64. Yuan, C.; Chen, W.; Pham, T.M.; Hao, H. Effect of aggregate size on bond behaviour between basalt fibre reinforced polymer sheets and concrete. *Composites. Part B Eng.* **2019**, *158*, 459–474. [[CrossRef](#)]
65. Soulioti, D.V.; Barkoula, N.M.; Paipetis, A.; Matikas, T.E. Effects of Fibre Geometry and Volume Fraction on the Flexural Behaviour of Steel-Fibre Reinforced Concrete. *Strain* **2011**, *47*, e535–e541. [[CrossRef](#)]
66. Bangi, M.R.; Horiguchi, T. Effect of fibre type and geometry on maximum pore pressures in fibre-reinforced high strength concrete at elevated temperatures. *Cem. Concr. Res.* **2012**, *42*, 459–466. [[CrossRef](#)]
67. Jansson, A.; Lofgren, I.; Lundgren, K.; Gylltoft, K. Bond of reinforcement in self-compacting steel-fibre-reinforced concrete. *Mag. Concr. Res.* **2012**, *64*, 617–630. [[CrossRef](#)]
68. Simões, T.; Octávio, C.; Valença, J.; Costa, H.; Dias-Da-Costa, D.; Júlio, E. Influence of concrete strength and steel fibre geometry on the fibre/matrix interface. *Composites. Part B Eng.* **2017**, *122*, 156–164. [[CrossRef](#)]
69. Susetyo, J. *Fibre Reinforcement for Shrinkage Crack Control in Prestressed, Precast Segmental Bridges*; University of Toronto: Toronto, ON, Canada, 2009.
70. Deluce, J.R. *Cracking Behaviour of Steel Fibre Reinforced Concrete Containing Conventional Steel Reinforcement*; University of Toronto: Toronto, ON, Canada, 2011.
71. Kim, J.H.J.; Park, C.G.; Lee, S.W.; Lee, S.W.; Won, J.P. Effects of the geometry of recycled PET fiber reinforcement on shrinkage cracking of cement-based composites. *Composites. Part B Eng.* **2008**, *39*, 442–450. [[CrossRef](#)]
72. Köksal, F.; Altun, F.; Yiğit, I.; Şahin, Y. Combined effect of silica fume and steel fiber on the mechanical properties of high strength concretes. *Constr. Build. Mater.* **2008**, *22*, 1874–1880. [[CrossRef](#)]
73. Nili, M.; Afroughsabet, V. Combined effect of silica fume and steel fibers on the impact resistance and mechanical properties of concrete. *Int. J. Impact Eng.* **2010**, *37*, 879–886. [[CrossRef](#)]
74. Mastali, M.; Dalvand, A. Use of silica fume and recycled steel fibers in self-compacting concrete (SCC). *Constr. Build. Mater.* **2016**, *125*, 196–209. [[CrossRef](#)]
75. Soetens, T.; Van Gysel, A.; Matthys, S.; Taerwe, L. A semi-analytical model to predict the pull-out behaviour of inclined hooked-end steel fibres. *Constr. Build. Mater.* **2013**, *43*, 253–265. [[CrossRef](#)]
76. Abdallah, S.; Fan, M.; Zhou, X. Effect of hooked-end steel fibres geometry on pull-out behaviour of ultra-high performance concrete. *World Acad. Sci. Eng. Technol. Int. J. Civ. Environ. Struct. Constr. Archit. Eng.* **2016**, *10*, 1530–1535.
77. Hao, Y.; Hao, H. Pull-out behaviour of spiral-shaped steel fibres from normal-strength concrete matrix. *Constr. Build. Mater.* **2017**, *139*, 34–44. [[CrossRef](#)]
78. Abdallah, S.; Rees, D.W.A. Comparisons Between Pull-Out Behaviour of Various Hooked-End Fibres in Normal-High Strength Concretes. *Int. J. Concr. Struct. Mater.* **2019**, *13*, 27. [[CrossRef](#)]
79. Khaloo, A.R.; Kim, N. Influence of concrete and fiber characteristics on behavior of steel fiber reinforced concrete under direct shear. *Aci Mater. J.* **1997**, *94*, 592–601.
80. Robins, P.; Austin, S.; Jones, P. Pull-out behaviour of hooked steel fibres. *Mater. Struct.* **2002**, *35*, 434–442. [[CrossRef](#)]
81. Anbukarasi, K.; Kalaiselvam, S. Study of effect of fibre volume and dimension on mechanical, thermal, and water absorption behaviour of luffa reinforced epoxy composites. *Mater. Eng.* **2015**, *66*, 321–330. [[CrossRef](#)]
82. Li, B.; Xu, L.; Shi, Y.; Chi, Y.; Liu, Q.; Li, C. Effects of fiber type, volume fraction and aspect ratio on the flexural and acoustic emission behaviors of steel fiber reinforced concrete. *Constr. Build. Mater.* **2018**, *181*, 474–486. [[CrossRef](#)]
83. Marar, K.; Eren, Ö.; Roughani, H. The influence of amount and aspect ratio of fibers on shear behaviour of steel fiber reinforced concrete. *KSCE J. Civ. Eng.* **2017**, *21*, 1393–1399. [[CrossRef](#)]
84. Sahin, Y.; Koksall, F. The influences of matrix and steel fibre tensile strengths on the fracture energy of high-strength concrete. *Constr. Build. Mater.* **2011**, *25*, 1801–1806. [[CrossRef](#)]
85. Boulekbache, B.; Hamrat, M.; Chemrouk, M.; Amziane, S. Influence of yield stress and compressive strength on direct shear behaviour of steel fibre-reinforced concrete. *Constr. Build. Mater.* **2012**, *27*, 6–14. [[CrossRef](#)]
86. Boulekbache, B.; Hamrat, M.; Chemrouk, M.; Amziane, S. Flexural behaviour of steel fibre-reinforced concrete under cyclic loading. *Constr. Build. Mater.* **2016**, *126*, 253–262. [[CrossRef](#)]
87. Wang, L.; Shen, N.; Zhang, M.; Fu, F.; Qian, K. Bond performance of Steel-CFRP bar reinforced coral concrete beams. *Constr. Build. Mater.* **2020**, *245*, 118456. [[CrossRef](#)]
88. Lee, S.-J.; Hong, Y.; Eom, A.-H.; Won, J.-P. Effect of steel fibres on fracture parameters of cementitious composites. *Compos. Struct.* **2018**, *204*, 658–663. [[CrossRef](#)]
89. Wu, Z.; Shi, C.; He, W.; Wu, L. Effects of steel fiber content and shape on mechanical properties of ultra high performance concrete. *Constr. Build. Mater.* **2016**, *103*, 8–14. [[CrossRef](#)]
90. *ACI 544.1R*; Report on Fiber Reinforced Concrete. American Concrete Institute-ACI Committee: Detroit, Michigan, 1996.
91. Wu, Z.; Shi, C.; Khayat, K.H. Investigation of mechanical properties and shrinkage of ultra-high performance concrete: Influence of steel fiber content and shape. *Composites. Part B Eng.* **2019**, *174*, 107021. [[CrossRef](#)]

92. Ashkezari, G.D.; Fotouhi, F.; Razmara, M. Experimental relationships between steel fiber volume fraction and mechanical properties of ultra-high performance fiber-reinforced concrete. *J. Build. Eng.* **2020**, *32*, 101613. [[CrossRef](#)]
93. Hoang, A.L.; Fehling, E. Influence of steel fiber content and aspect ratio on the uniaxial tensile and compressive behavior of ultra high performance concrete. *Constr. Build. Mater.* **2017**, *153*, 790. [[CrossRef](#)]
94. Guneyisi, E.; Gesoglu, M.; Ipek, S. Effect of steel fiber addition and aspect ratio on bond strength of cold-bonded fly ash lightweight aggregate concretes. *Constr. Build. Mater.* **2013**, *47*, 358–365. [[CrossRef](#)]
95. Zhang, L.; Liu, J.; Liu, J.; Zhang, Q.; Han, F. Effect of Steel Fiber on Flexural Toughness and Fracture Mechanics Behavior of Ultrahigh-Performance Concrete with Coarse Aggregate. *J. Mater. Civ. Eng.* **2018**, *30*, 04018323. [[CrossRef](#)]
96. Dupont, D.; Vandewalle, L. Distribution of steel fibres in rectangular sections. *Cem. Concr. Compos.* **2005**, *27*, 391–398. [[CrossRef](#)]
97. Huang, H.; Gao, X.; Li, L.; Wang, H. Improvement effect of steel fiber orientation control on mechanical performance of UHPC. *Constr. Build. Mater.* **2018**, *188*, 709–721. [[CrossRef](#)]
98. Soroushian, P.; Lee, C.-D. Distribution and orientation of fibers in steel fiber reinforced concrete. *Mater. J.* **1990**, *87*, 433–439.
99. Laranjeira, F.; Grünwald, S.; Walraven, J.; Blom, C.; Molins, C.; Aguado, A. Characterization of the orientation profile of steel fiber reinforced concrete. *Mater. Struct.* **2011**, *44*, 1093–1111. [[CrossRef](#)]
100. Mudadu, A.; Tiberti, G.; Germano, F.; Plizzari, G.A.; Morbi, A. The effect of fiber orientation on the post-cracking behavior of steel fiber reinforced concrete under bending and uniaxial tensile tests. *Cem. Concr. Compos.* **2018**, *93*, 274–288. [[CrossRef](#)]
101. Nieuwoudt, P.D.; Boshoff, W.P. Time-dependent pull-out behaviour of hooked-end steel fibres in concrete. *Cem. Concr. Compos.* **2017**, *79*, 133–147. [[CrossRef](#)]
102. Marcos-Meson, V.; Solgaard, A.; Fischer, G.; Edvardsen, C.; Michel, A. Pull-out behaviour of hooked-end steel fibres in cracked concrete exposed to wet-dry cycles of chlorides and carbon dioxide—Mechanical performance. *Constr. Build. Mater.* **2020**, *240*, 117764. [[CrossRef](#)]
103. de Oliveira, F.L. *Design-Oriented Constitutive Model for Steel Fiber Reinforced Concrete*; Universitat Politècnica de Catalunya: Barcelona, Spain, 2010.
104. Marković, I. *High-Performance Hybrid-Fibre Concrete: Development and Utilisation*; IOS Press: Amsterdam, The Netherlands, 2006.
105. Breitenbücher, R.; Meschke, T.G.; Song, M.F.; Zhan, M.Y. Experimental, analytical and numerical analysis of the pullout behaviour of steel fibres considering different fibre types, inclinations and concrete strengths. *Struct. Concr.* **2014**, *15*, 126–135. [[CrossRef](#)]
106. Abdallah, S.; Fan, M.; Zhou, X. Pull-Out Behaviour of Hooked End Steel Fibres Embedded in Ultra-high Performance Mortar with Various W/B Ratios. *Int. J. Concr. Struct. Mater.* **2017**, *11*, 301–313. [[CrossRef](#)]
107. Thomas, J.; Ramaswamy, A. Mechanical Properties of Steel Fiber-Reinforced Concrete. *J. Mater. Civ. Eng.* **2007**, *19*, 385–392. [[CrossRef](#)]
108. Silva, F.d.A.; Mobasher, B.; Filho, R.D.T. Cracking mechanisms in durable sisal fiber reinforced cement composites. *Cem. Concr. Compos.* **2009**, *31*, 721–730. [[CrossRef](#)]
109. Pujadas, P.; Blanco, A.; Cavalaro, S.H.P.; De La Fuente, A.; Aguado, A. The need to consider flexural post-cracking creep behavior of macro-synthetic fiber reinforced concrete. *Constr. Build. Mater.* **2017**, *149*, 790–800. [[CrossRef](#)]
110. Llano-Torre, A.; Arango, S.E.; García-Taengua, E.; Martí-Vargas, J.R.; Serna, P. Influence of fibre reinforcement on the long-term behaviour of cracked concrete. In *Creep Behaviour in Cracked Sections of Fibre Reinforced Concrete*; Springer: Berlin/Heidelberg, Germany, 2017; pp. 195–209.
111. García-Taengua, E.; Mas, L.; Martí Vargas, J.R.; Ros, P.S. New Views on the Study of Variables Affecting Bond of Reinforcing Bars to Steel Fiber Reinforced Concrete. In Proceedings of the 8th RILEM International Symposium on Fibre Reinforced Concrete: Challenges and Opportunities (BEFIB 2012), Guimarães, Portugal, 19–21 September 2012; RILEM Publications SARL: Marne, France, 2012.
112. Torre-Casanova, A.; Jason, L.; Davenne, L.; Pinelli, X. Confinement effects on the steel–concrete bond strength and pull-out failure. *Eng. Fract. Mech.* **2013**, *97*, 92–104. [[CrossRef](#)]
113. Tattersall, G.; Urbanowicz, C. Bond strength in steel-fibre-reinforced concrete. *Mag. Concr. Res.* **1974**, *26*, 105–113. [[CrossRef](#)]
114. Chan, Y.-W.; Chu, S.-H. Effect of silica fume on steel fiber bond characteristics in reactive powder concrete. *Cem. Concr. Res.* **2004**, *34*, 1167–1172. [[CrossRef](#)]
115. Nazarimofrad, E.; Shaikh, F.U.A.; Nili, M. Effects of steel fibre and silica fume on impact behaviour of recycled aggregate concrete. *J. Sustain. Cem. Based Mater.* **2017**, *6*, 54–68. [[CrossRef](#)]
116. Shaikh, F.U.A.; Shafaei, Y.; Sarker, P.K. Effect of nano and micro-silica on bond behaviour of steel and polypropylene fibres in high volume fly ash mortar. *Constr. Build. Mater.* **2016**, *115*, 690–698. [[CrossRef](#)]
117. Xu, L.; Wu, F.; Chi, Y.; Cheng, P.; Zeng, Y.; Chen, Q. Effects of coarse aggregate and steel fibre contents on mechanical properties of high performance concrete. *Constr. Build. Mater.* **2019**, *206*, 97. [[CrossRef](#)]
118. Huang, C.; Zhao, G. Properties of steel fibre reinforced concrete containing larger coarse aggregate. *Cem. Concr. Compos.* **1995**, *17*, 199–206. [[CrossRef](#)]
119. Liu, J.; Han, F.; Cui, G.; Zhang, Q.; Lv, J.; Zhang, L.; Yang, Z. Combined effect of coarse aggregate and fiber on tensile behavior of ultra-high performance concrete. *Constr. Build. Mater.* **2016**, *121*, 310–318. [[CrossRef](#)]
120. Larsen, I.L.; Thorstensen, R.T. The influence of steel fibres on compressive and tensile strength of ultra high performance concrete: A review. *Constr. Build. Mater.* **2020**, *256*, 119459. [[CrossRef](#)]

121. Song, P.S.; Hwang, S. Mechanical properties of high-strength steel fiber-reinforced concrete. *Constr. Build. Mater.* **2004**, *18*, 669–673. [[CrossRef](#)]
122. Ding, Y.; You, Z.; Jalali, S. The composite effect of steel fibres and stirrups on the shear behaviour of beams using self-consolidating concrete. *Eng. Struct.* **2011**, *33*, 107–117. [[CrossRef](#)]
123. Eren, Ö.; Marar, K. Effects of limestone crusher dust and steel fibers on concrete. *Constr. Build. Mater.* **2009**, *23*, 981–988. [[CrossRef](#)]
124. Köksal, F.; Şahin, Y.; Gencel, O.; Yiğit, I. Fracture energy-based optimisation of steel fibre reinforced concretes. *Eng. Fract. Mech.* **2013**, *107*, 29–37. [[CrossRef](#)]
125. Shafaei, Y.; Shaikh, F.U.A.; Sarker, P.K. Effect of the Fibre Geometry on Pull-out Behaviour of HVFA Mortar Containing Nanosilica. *Procedia Eng.* **2017**, *171*, 1535–1541. [[CrossRef](#)]
126. Abdallah, S.; Fan, M.; Rees, D.W.A. Analysis and modelling of mechanical anchorage of 4D/5D hooked end steel fibres. *Mater. Des.* **2016**, *112*, 539–552. [[CrossRef](#)]
127. Afroughsabet, V.; Biolzi, L.; Ozbakkaloglu, T. High-performance fiber-reinforced concrete: A review. *J. Mater. Sci.* **2016**, *51*, 6517–6551. [[CrossRef](#)]
128. Zain, M.; Mahmud, H.; Ilham, A.; Faizal, M. Prediction of splitting tensile strength of high-performance concrete. *Cem. Concr. Res.* **2002**, *32*, 1251–1258. [[CrossRef](#)]
129. Li, Z. *Advanced Concrete Technology*; Wiley: Hoboken, NJ, USA, 2011.
130. Alhozaimy, A.M.; Soroushian, P.; Mirza, F. Mechanical properties of polypropylene fiber reinforced concrete and the effects of pozzolanic materials. *Cem. Concr. Compos.* **1996**, *18*, 85–92. [[CrossRef](#)]
131. Hsie, M.; Tu, C.; Song, P.S. Mechanical properties of polypropylene hybrid fiber-reinforced concrete. *Mater. Sci. Eng. A Struct. Mater. Prop. Microstruct. Process* **2008**, *494*, 153–157. [[CrossRef](#)]
132. Oluokun, F.A.; Burdette, E.G.; Deatherage, J.H. Splitting tensile-strength and compressive strength relationship at early ages. *Aci Mater. J.* **1991**, *88*, 115–121.
133. Choi, Y.; Yuan, R.L. Experimental relationship between splitting tensile strength and compressive strength of GFRC and PFRC. *Cem. Concr. Res.* **2005**, *35*, 1587–1591. [[CrossRef](#)]
134. Murali, G.; Santhi, A.S.; Ganesh, G.M. Impact resistance and strength reliability of fiber reinforced concrete using two parameter weibull distribution. *J. Eng. Appl. Sci.* **2014**, *9*, 554–559.
135. Lu, X.; Hsu, C.-T.T. Behavior of high strength concrete with and without steel fiber reinforcement in triaxial compression. *Cem. Concr. Res.* **2006**, *36*, 1679–1685. [[CrossRef](#)]
136. Sivakumar, A.; Santhanam, M. Mechanical properties of high strength concrete reinforced with metallic and non-metallic fibres. *Cem. Concr. Compos.* **2007**, *29*, 603–608. [[CrossRef](#)]
137. Wang, H.T.; Wang, L.C. Experimental study on static and dynamic mechanical properties of steel fiber reinforced lightweight aggregate concrete. *Constr. Build. Mater.* **2013**, *38*, 1146–1151. [[CrossRef](#)]
138. Yazıcı, Ş.; İnan, G.; Tabak, V. Effect of aspect ratio and volume fraction of steel fiber on the mechanical properties of SFRC. *Constr. Build. Mater.* **2007**, *21*, 1250–1253. [[CrossRef](#)]
139. Abbass, W.; Khan, M.I.; Mourad, S. Evaluation of mechanical properties of steel fiber reinforced concrete with different strengths of concrete. *Constr. Build. Mater.* **2018**, *168*, 556. [[CrossRef](#)]
140. Yap, S.P.; Bu, C.H.; Alengaram, U.J.; Mo, K.H.; Jumaat, M.Z. Flexural toughness characteristics of steel–polypropylene hybrid fibre-reinforced oil palm shell concrete. *Mater. Eng.* **2014**, *57*, 652–659. [[CrossRef](#)]
141. Mo, K.H.; Yap, K.K.Q.; Alengaram, U.J.; Jumaat, M.Z. The effect of steel fibres on the enhancement of flexural and compressive toughness and fracture characteristics of oil palm shell concrete. *Constr. Build. Mater.* **2014**, *55*, 20–28. [[CrossRef](#)]
142. Wang, J.-Y.; Chia, K.-S.; Liew, R.; Zhang, M.-H. Flexural performance of fiber-reinforced ultra lightweight cement composites with low fiber content. *Cem. Concr. Compos.* **2013**, *43*, 39–47. [[CrossRef](#)]
143. Balaguru, R.; Najm, H. High-performance fiber-reinforced concrete mixture proportions with high fiber volume fractions. *Aci Mater. J.* **2004**, *101*, 281–286.
144. Soroushian, P.; Bayasi, Z. Fiber type effects on the performance of steel fiber reinforced concrete. *Mater. J.* **1991**, *88*, 129–134.
145. Abu-Lebdeh, T.; Hamoush, S.; Heard, W.; Zornig, B. Effect of matrix strength on pullout behavior of steel fiber reinforced very-high strength concrete composites. *Constr. Build. Mater.* **2011**, *25*, 39–46. [[CrossRef](#)]
146. Isla, F.; Ruano, G.; Luccioni, B. Analysis of steel fibers pull-out. Experimental study. *Constr. Build. Mater.* **2015**, *100*, 183–193. [[CrossRef](#)]